SHELL MIDDLE DISTILLATE SYNTHESIS: THE PROCESS, THE PLANT, THE PRODUCTS

Peter J. A. Tijm
Shell International Gas Ltd.
Shell Centre, Downstream Building
London SE1 7NA, U.K.

Keywords: natural gas conversion, Shell Middle Distillate Synthesis, Fischer-Tropsch

INTRODUCTION

The importance of natural gas as a source of energy has increased substantially in recent years and is expected to continue to increase. As a result of the frantic search for oil set off by the oil shocks of the early and late 1970s, many new gas fields were discovered around the world, leading to a dramatic increase in the proven world gas reserves. This growth in gas reserves is still continuing today and despite the low oil prices, the world proven gas reserves have been growing at a rate which is twice the current world natural gas consumption rate. Proven world gas reserves are now approaching those of oil and, on the basis of the current reserves situation and relative depletion rates, natural gas seems to be set to outlast oil.

Notwithstanding the growing importance of natural gas, its main drawback remains its low energy density, which makes its transportation to the point of use expensive and which, in the case of remote gas, may even prohibit its exploration and for development. Liquefaction is a way to overcome this problem and various liquefied natural gas (LNG) projects have already been realized around the world.

Recognizing the growing importance of natural gas, Shell has been looking at other ways of using natural gas profitably, particularly those reserves which are remote from the market. The key element is in the transportation aspect and so cost improvements to conventional pipeline and LNG schemes are being studied. However, where such schemes will continue to make an important contribution to the natural gas trade, their end products (natural gas) are by nature confined to markets for natural gas. Shell has therefore also been looking at processes that chemically convert natural gas into liquid hydrocarbons. Using such processes not only reduces the transportation costs substantially, but also a much larger market becomes available, especially if these hydrocarbons are transport fuels. Moreover, apart from providing a means to commercialize remote gas reserves, this could also serve to reduce the reliance on oil or oil-product imports and perhaps as important, save on foreign exchange.

The foregoing underlines Shell's strategy in the natural gas business:

1. Bring gas to the market.
2. Bring value to the product.

It has been realized that there are many places in the world where gas is available, without a ready market and where, as a consequence, it would have a much lower intrinsic value compared with transportation fuels. It is this difference in value that would drive a synthetic fuel project and provide opportunities for both government and private enterprises.

The present scene in the field of oil and transportation fuels and the prospects for the near and medium term, however, call for a careful and selective approach to any synfuel development. At current oil prices almost no alternative energy technology can compete with existing refining. On the other hand, the crises of the early seventies and early eighties provided important lessons: emergencies come at relatively short notice, and, because of the lead times usually involved in technological development, in a crisis the answers to problems always come too late.

Next to the synthetic hydrocarbon transportation fuels, a similar role could be perceived for methanol. However, use of methanol as a transport fuel, either as M85 or neat methanol, has considerable drawbacks. These include the required modifications to fuel distribution systems and to car/engine fuel systems. Synthetic hydrocarbons, on the other hand, have the advantage that they can be readily incorporated into existing fuels which can be used in existing equipment. In addition, middle distillates manufactured from natural gas have very environmentally friendly properties, upon which we will elaborate in this paper. The cleanliness of natural gas is, as it were, transferred into its products. The middle distillates from SMDS will therefore be extremely well positioned in the market place.

THE PROCESS

The SMDS process consists of three stages:

1. Syngas manufacturing

2. Heavy Paraffin Synthesis (HPS)
3. Heavy Paraffin Conversion (HPC)

The overall process starts with the conversion of natural gas into synthesis gas, for which there are several commercial processes available. For the production of predominantly saturated hydrocarbons, $-(CH_2)-$, the syngas components H_2 and CO, are consumed in a molar ratio of about 2:1, so a production in about that ratio is desirable. This influences the choice of process, as will be explained below.

The next step of the process, the hydrocarbon synthesis, is, in fact, a modernized version of the classical Fischer-Tropsch (FT) process, with the emphasis on high yields of useful products. The Fischer-Tropsch process developed by Shell for SMDS favors the production of long chain waxy molecules which, as such, are unsuitable for transportation fuels. The hydrocarbon synthesis step is therefore followed by a combined hydro-isomerization and hydrocracking step to produce the desired, lighter products. By opting for the production of waxy molecules in the Fischer-Tropsch step, the amount of unwanted smaller hydrocarbons or gaseous products, produced as by-products, is substantially reduced. This means that the process, contrary to the old 1930's Fisher-Tropsch technology, can be fuel balanced and does not make "gas" out of gas. Combined with the high selectivity towards middle distillates in the hydrocracking step this leads to a very high overall yield of product in the desired range.

In the final stage of the process, the products, mainly kerosene, gas oil and some naphtha, are separated by distillation. By judicious selection of the severity of the hydrocracking reaction and the cut-points, the product slate can be biased towards kerosene or towards gas oil.

Synthesis Gas Manufacture

For the production of synthesis gas in principle two technologies are available, viz., steam reforming and partial oxidation.

Steam Reforming (SMR)

Starting from pure methane, SMR is the most commonly used conversion process, and could theoretically produce a synthesis gas with an H_2/CO ratio of about 3. However, as a result of the occurring CO - shift, more H_2 is produced and this ratio will be in the range of 5-7 rather than 3.

Because the H2/CO ratio in the synthesis gas is greater than 2, in the subsequent hydrocarbon synthesis step less hydrogen will be consumed than is produced in the syngas step. This means that steam reforming always results in the production of excess H_2. An often practiced solution is to burn the surplus hydrogen in the reforming furnace. This means, however, that part of the synthesis gas is used as fuel. Another disadvantage is that the maximum SMR pressure is about 30 bar, while the Fischer-Tropsch reaction is preferably carried out at somewhat higher pressures.

Partial Oxidation

A synthesis gas suitable for the production of middle distillates, with a H_2/CO ratio of about 2, can be produced by partial oxidation:

$$2\ CH_4 + O_2 \text{ ----> } 2\ CO + 4\ H_2$$

For partial oxidation with pure oxygen, an excellent eligible process is the Shell Gasification Process (SGP). The question, whether the costs involved with the production of a gas with the wrong H2/CO ratio, as in the case of steam reforming, are not substantially smaller than the cost required for the production of pure oxygen, has been answered in favor of the SGP process combined with modern oxygen technology.

For the Fischer-Tropsch type of catalysts, the synthesis gas must be completely free of sulphur. For this requirement, it has been found to be economical to remove all sulphur components upstream of the partial oxidation step for which, in principle, a number of well-known treating processes are available. In practice, zinc oxide beds are employed, to remove the last traces of sulphur and to act as an absolute safeguard.

The Hydrocarbon Synthesis Step

In the next step, the synthesis gas is converted into long chain, heavy paraffins, and this step is therefore called the Heavy Paraffin Synthesis (HPS) step, the heart of the SMDS process. In this step the reaction mechanism follows the well-known Schultz-Flory polymerization kinetics, which are characterized by the probability of chain growth (α) vs. chain termination ($1-\alpha$). There is always a regular molecular mass distribution in the total product and a high

alpha, corresponds with a high average molecular molecular mass of the paraffinic product. The paraffinic hydrocarbons produced via the FT reaction are highly linear. This implies that the synthesis reaction can be regarded as a stepwise addition of a C1 segment to the end of an existing chain. Since atoms of the alkyl chain remote from the end will hardly be capable of influencing this reaction, it is plausible that the relative probabilities of chain growth and chain termination will be independent of the length of the alkyl chain. The carbon number distribution of the FT product can therefore be described fairly accurately by a simple statistical model with as a single parameter (the Anderson Flory-Schultz [AFS] distribution, the value of being dependent upon the catalyst and reaction conditions. In a few hundred formulations under different operating conditions it was confirmed that the carbon number distributions were in close agreement with the AFS chain growth kinetics discussed above, with values varying between 0.70 and 0.95

The above feature implies, however, that the FT process will yield either large amounts of gaseous hydrocarbons such as methane, or products which have a very wide carbon number distribution. Theoretically, only methane can be produced with 100% selectively. All other products including fractions boiling in specific ranges, such as gasoline, kerosene and gas oil, can be produced only with relatively low selectivities. The only product fraction, beside light gases, which can be produced with high selectivity is heavy paraffin wax. It is for this reason that the synthesis part of the SMDS process has been designed to produce a long-chain hydrocarbon wax.

During the reaction: $2\ H_2 + CO \text{ ----> } H_2O + -(CH_2)-$ an appreciable amount of heat is released. For the classical catalyst system, this requires a considerable control of the temperature in view of the following constraints:

- The temperature window of stable operation is rather small
- A high space-time yield demands a high temperature
- At only moderately higher temperature a side reaction leading to methane formation becomes more dominant, reducing selectivity and, eventually, stability.

Because of these shortcomings, Shell has developed a new and proprietary catalyst system, which establishes substantial improvements in all these areas. Its robustness allows the use of a fixed bed pipe reactor system at a temperature level where heat recovery, via production of steam, leads to an efficient energy recovery. The catalyst, which is regenerable (cycle > 1 year) has an expected useful life of well over five years.

Heavy Paraffin Conversion (HCP)

One of the prerequisites for attaining a high selectivity towards middle distillates is a sufficiently high average molecular weight of the raw product. This product, which is predominantly waxy but contains small amounts of olefins and oxygenates, has to be isomerized and cleaned up, while little hydrocracking should take place concurrently. A commercial Shell catalyst is used in a trickle-flow reactor as is employed in refinery hydrocracking operations, but under rather mild conditions of pressure and temperature.

An important observation in this respect is the carbon number distribution of the total product obtained after hydro-cracking of a Fischer-Tropsch fraction containing normal paraffins. As an example the product distribution after cracking n-hexadecane shows that very little methane and ethane, if any at all, is formed. In addition, process conditions can be chosen such as to allow partial evaporation of the lighter hydrocarbons so that they escape easily from the reactor. Since the heavier paraffins may then preferentially condense or absorb on the catalyst surface, they will remain longer in the reactor and thus have a better chance to react. Initially, one might expect the curve to follow an approximately exponential increase with an increase in carbon number as the absorption coefficient is an exponential function of the heat of absorption, while this heat of absorption for normal paraffins is known to increase about linearly with increasing carbon number. The increment per carbon number amounts to some 10-15 kJ/mol. Above a certain chain length, however, one may expect the effect to level out as the degree of absorption approaches 100%. The result would be a chain-length-dependent reactivity, which shows a very steep increase in the lower carbon number range and an about linear increase in for the higher carbon numbers.

Taking this into account and assuming an equimolar production ratio for all cracked components except for those resulting from breakage of the first three bonds, one can calculate that a C-20 paraffin can be converted into some 80% wt of C-10 - C-20 material, while only some 20% wt ends up in the lighter fraction.

The principle of combining the length-independent chain growth process with a selective, chain-length dependent conversion process has been applied to selectively produce middle distillate paraffins from synthesis gas. To take full advantage of this concept, the Fischer-Tropsch catalyst and the operating conditions were chosen as to produce a heavy product with a high alpha-value, minimizing the formation of undesired light hydrocarbons. The

effectiveness of the two stage approach also creates flexibility creating selective distributions of Fischer-Tropsch liquid products after heavy paraffin conversion at different cracking severities.

The HPC product is subsequently fractionated in a conventional distillation section. The product fraction which is still boiling above the gas oil range is recycled to the HPC section. By varying the process severity or the conversion per pass one can influence the selectivity towards a preferred product. Hence one may opt for a kerosene mode of operation yielding some 50% kerosene on total liquid product or for a gas oil mode of operation producing some 60% gas oil. In practice the following variability has been proven:

% wt	Gas Oil mode	Kerosene mode
Tops/naphtha	15	25
Kerosene	25	50
Gas Oil	60	25

Compared to syngas requirements of the total complex, the hydrogen demand for the HPC step is very modest. This hydrogen can be recovered from a slipstream of the syngas via any of several methods; one modern method makes use of membranes. Steam reforming of the synthesis purge gas and/or natural gas is also a possibility.

THE PLANT

Shell, together with its partners Petronas, Sarawak State Government and Mitsubishi Corporation, are the shareholders in the first commercial SMDS plant in Bintulu, Malaysia, adjacent to the Malaysia LNG plant. The plant will convert 100 million cubic ft/day of natural gas from offshore fields into approximately 500,000 metric tons/year of hydrocarbons. The Malaysian SMDS project, based on the conversion of natural gas to transportation fuels, like kerosene and gas oil, has through its development and in particularly the efforts spent at Shell's Research Laboratories, gained new grounds. For petrochemicals, the ability to produce naphtha as chemical feedstock is a further advantage. The tops/naphtha fraction is completely paraffinic and therefore makes an ideal cracker feedstock for ethylene manufacture. Obviously, taking into account the paraffinic nature of the hydrocarbons specific solvents provide another market opportunity for the SMDS products.

Further more the SMDS Bintulu project has taken advantage of producing high quality waxes by diverting part of the HPS product stream to the Wax Production Unit. After a hydrogenation step the C17 minus fraction is distilled off in various distillation columns. Subsequently, the various wax qualities are produced by further distillation. The wax grades are either produced and transported as bulk liquids or as solids, in which case transportation will take place in containers, in the form of slabs or granulates.

Since November 1989 when the ground breaking ceremony took place, there has been a flurry of activities: detailed engineering, ordering of critical equipment, recruitment and training, formation of the start-up and operating crew, construction, commissioning and start-up. Construction was completed by end 1992. Commissioning of a complex plant, introducing new technology, is a time-consuming exercise. Starting with the pre-commissioning in December 1992, it has been progressing in the first quarter of 1993. As a result, in the second quarter of 1993 the first middle distillates were produced.

THE PRODUCT

As can be expected from a Fischer-Tropsch process of this type, products manufactured by the SMDS process are completely paraffinic and free from nitrogen and sulphur. Both the kerosene and gas oil have excellent combustion properties, as the typical product data, given below, show. In this paper particular focus will be given to the excellent properties of the SMDS gas oil and its potential in the market.

	SMDS Gas Oil	CARB Specs.	CEN Specs.
Cetane number	76	40 min	49 min
Density (kg/cu.m)	780	N/S	820-860
Sulphur (ppm)	zero	500	500 (1996)
Aromatics (% m/m)	zero	10 max	N/S
Cloud point (deg. C)	1	-5	N/S
CFPP (deg. C)	-2	N/S	+5 to -20*
Distillation:			
90% recovery (deg. C)	340	288-338	
95% recovery (deg. C)	350		370 max

* depending on climatic band chosen

Because of these excellent properties, which are far in excess of the minimum specifications in terms of smoke point and cetane number, these products make excellent blending components for upgrading of lower-quality stock derived from catalytic and thermal cracking operations; for example cycle oils. Alternatively the products could enter in a market where premium specifications are valued to meet local requirements. Examples include the California diesel market, where the California Air Resources Board (CARB) has imposed a fuel specification with low sulphur and aromatics and the Committee for European Norms (CEN) which has established a fairly high cetane number requirement.

OUTLOOK

As is well known, capital and operating costs for synfuel complexes are highly dependent on location and product slate produced. It has been found that the specific capital cost of a 10,000 bbl/d plant built on a developed site in an industrialized country would be around US$ 30,000 per daily barrel, whereas for a similar plant in a remote and undeveloped location the cost could be up to double that amount. The uniqueness of the SMDS products, though, including their added value, gives the SMDS process excellent opportunities to provide return on investment.

If feedstock is natural gas priced at US$ 0.5/MMBtu, the feedstock cost element in the product is about US$ 5/bbl. The total fixed and other variable operating costs are estimated at a further US$ 5/bbl. The total required selling price for the product will depend on numerous factors, including fiscal regimes, local incentives, debt/equity ratio, type of loans and corporate return requirements. The premium that may be realized for the high quality products is also a locally influenced and important aspect; it may be as high as 6-8 US$/bbl over and above the normal straight run middle distillate value.

Another important factor is whether the products are for inland use or for export. For countries with sufficient gas, but that need to import oil or oil products to meet their local demand, SMDS products manufactured in that country should realize at least, import parity values. In some cases these may be far above the normal world spot market values. For such countries therefore, the national benefit of the SMDS process may be substantial.

In addition to these factors, the capacity of the plant is of great importance. Especially for remote locations, where self-sufficiency of the plant is essential, larger plants, in the 25,000 to 50,000 bbl/d range, have a much better economy of scale. Moreover, whilst the process is ready for commercialization, further developments are underway, directed at increasing the efficiency of the process even further and reducing the capital cost. An important area for these efforts is the synthesis gas manufacturing plant, which constitutes more than 50% of the total process capital cost. Other fields of interest include further catalyst improvement, the design of the synthesis reactors and general process integration within the project. It is expected that work in this area combined with further improvements for larger size plants, will bring the specific capital costs for remote areas to the range of US$25,000 to 30,000/daily barrel.

SMDS technology has been developed to a stage where it can be considered as technically proven and, subject to local circumstances, commercially viable. Installation of SMDS plants can bring significant national benefits to countries with uncommitted gas reserves, either through export from the plant or inland use of the products, thereby reducing the need to import oil and oil products and saving on foreign exchange.

REFERENCES

Eilers, J., Posthuma, S.A, and Sie, S.T., (1990), 'The Shell Middle Distillate Process (SMDS)', paper presented at the AIChE Spring National Meeting, Orlando, Florida, USA, March 18-20.

Oerlemans, T.W., Van Wechem, H.M.H., and Zuideveld, P.L., (1991), 'Conversion of Natural Gas to Middle Distillates via the SMDS Process', paper presented at the 18th World Gas Conference, Berlin, FRG, July 8-11.

Tijm, P.J.A., Van Wechem, H.M.H., and Senden, M.M.G., (1993),'New Opportunities for Marketing Natural Gas: The Shell Middle Disillate Synthesis Process', paper presented at the GASTECH 93, 15th International LNG/LPG Conference & Exhibition, Paris, February 16-19.

PRODUCT VALUATION OF FISCHER-TROPSCH DERIVED FUELS

John J. Marano, Burns and Roe Services Corp.
Shelby Rogers, U.S. Department of Energy
Pittsburgh Energy Technology Center
Pittsburgh, PA 15236

Gerald N. Choi, Bechtel Corp.
P.O. Box 193965, San Francisco, CA 94119

Sheldon J. Kramer, Amoco Oil Company
P.O. Box 3011, Naperville, IL 60566

Keywords: Fischer-Tropsch, Linear Programming, Clean Air Act

INTRODUCTION

The Clean Air Act Amendments (CAAA) of 1990 have placed stringent requirements on the quality of transportation fuels. Most petroleum refiners are scrambling to meet provisions of the Amendments to be implemented between 1995 and 2000. These requirements will also have significant implications for the production of alternative fuels. These have been examined for Fischer-Tropsch (F-T) derived fuels.

This analysis was conducted in conjunction with the U.S. Department of Energy (DOE) sponsored project, **Baseline Design/Economics for Advanced Fischer-Tropsch Technology**, conducted by Bechtel and Amoco[1,2]. The goal of this study was to develop a baseline design for indirect liquefaction of Illinois No. 6 coal using gasification, syngas conversion in slurry reactors with iron catalysts, and conventional refinery upgrading of the F-T derived hydrocarbon liquids. One alternative case using ZSM-5 upgrading technology[3] was also considered. This study included complete capital and operating cost estimates for the processes.

To perform economic analyses for the different design cases, the products from the liquefaction plant had to be valued relative to conventional transportation fuels. This task was accomplished by developing a Linear Programming (LP) model for a typical midwest refinery, and then feeding the F-T liquids to the refinery. In this way, the breakeven value determined for these materials is indicative of the price they could command if available in the marketplace.

Inputs to the LP model include: refinery size, configuration, feedstocks, products, specifications, prices, and operating and capital recovery costs. The model was set up to be representative of conditions anticipated for the turn of the century. This required inclusion of fuel specifications from the CAAA of 1990 which have or will come into force by the year 2000.

CAAA FUEL SPECIFICATIONS

Meeting the requirements of the 1990 CAAA have been the subject of negotiations between the government, the refining and transportation industries, and various environmental groups. At the time this study was conducted, agreement had only been reached in regards to fuel requirements up through 1995. Reduced summer gasoline volatility (RVP), a winter oxygenated gasoline program for CO non-attainment areas, and a low sulfur diesel program already have been implemented. A federal Phase I reformulation program is scheduled for implementation in 1995. It requires the production of reformulated gasoline for severe ozone non-attainment areas of the country.

The ultimate goal of the CAAA fuels program is the reduction of gasoline volatility, toxicity, and (more recently) NOx to below 1990 levels. These reduction goals are to be phased-in between 1995 and the year 2000 under the federal Phase II reformulation program. In December 1993, the U.S. Environmental Protection Agency published a first draft of the Complex Model which must be used by refiners before 2000 to establish reduction targets.

In addition to the federally mandated programs, California, through the California Air Resources Board (CARB), has promulgated its own Phase I and Phase II programs. In general, the requirements of the CARB programs are more strict than the federal programs. Fuels marketed in California will need to satisfy both the federal and CARB requirements. The CARB Phase I program coincides with the federal program, whereas the CARB Phase II program is to be implemented in 1996. The significance of the California programs is that the rest of the nation has in the past followed California's lead in setting environmental policy. Thus, many of CARB's more severe requirements could become effective nationwide sometime early in the next century.

At the time this study was conducted, little was known regarding the federal Phase II program. Therefore, two different scenarios were modeled with the LP spanning a range of possibilities. The first scenario (Scenario I) assumes fuel specifications in accordance with the federal Phase I program, and the second scenario assumes specifications similar to the CARB Phase II program. Table 1 lists key fuel specifications for gasoline and diesel fuel under the two scenarios.

LP MODELING

The crude capacity of the typical midwest refinery was set at 150,000 bbl/day for this study. A composite crude with an API gravity of 32.9° and total sulfur content of 1.30 wt% was used as the basis for the comparisons with F-T liquids. These properties were projected by extrapolating historical crude quality trends. The crude oil was given a nominal price of $18 per bbl. Product values were based on current margins between crude and finished products and forecasts for incremental margins due to fuel reformulation. Product demands also were forecast for the year 2000. Table 2 lists the product rates used in the study.

Capital expansions will be required by U.S. refineries to make the fuels required by the CAAA. These were estimated in order to establish the base refinery configuration for the year 2000 and also to determine if any capital savings could be achieved from blending F-T derived fuels with their petroleum counterparts. Table 2 shows a comparison of the typical midwest refinery circa. 1990 and 2000.

Table 2 shows that major expansion of refinery hydrotreating capacity will be needed to meet both reduced gasoline and reduced diesel sulfur limits. Associated with the increase in hydrotreating are increases in hydrogen production and sulfur recovery. Producing oxygenated gasoline will require the addition of MTBE (methyl tert-butyl ether) and TAME (tert-amyl methyl ether) units. These ethers are produced from purchased methanol and isobutylene and isoamylene available within the refinery from the catalytic cracking and delayed coking operations. Supplemental n-butane will also be purchased and converted to isobutylene to supply additional MTBE. Benzene levels in gasoline will be controlled by dehexanizing the catalytic reformer feed to remove benzene and its precursors.

F-T PRODUCT DESCRIPTION

The indirect liquefaction designs discussed above produce two distinct product slates. These are listed in the footnote beneath Table 3. For the most part, these streams have been fully upgraded at the liquefaction plant and are suitable for blending to finished fuels. Important properties of these blending components are shown in Table 3. These properties were estimated based on available data from previous DOE-sponsored projects[1].

In the baseline design, conventional upgrading of F-T liquids produces about one barrel of gasoline for every barrel of diesel. The components of the gasoline are alkylate, isomerate and reformate. These materials are essentially equivalent to their petroleum counterparts produced in a typical refinery. Alkylate, produced from reacting C3, C4, and C5 olefins with isobutane, is the highest octane component in the gasoline. Isomerate is produced from isomerizing normal pentane and hexane. It has a moderate octane rating but is relatively volatile. The reformate, on the other hand, has a high octane rating but contains undesirable aromatic components. The benzene content of the reformate is low due to the dehexanizing of the reformer feed. All of the gasoline blending components have zero sulfur and olefins, which is of considerable benefit when manufacturing CAAA mandated fuels.

Diesel produced from conventional upgrading of F-T products consists of hydrotreated straight-run distillate blended with distillate from wax hydrocracking. The F-T diesel has rather unique properties relative to petroleum-derived diesels. It is sulfur free, almost completely paraffinic, and has an extremely high cetane rating.

The alternative upgrading case using ZSM-5 produces a gasoline-to-diesel ratio of about 1.8, which is more typical of the U.S. transportation fuels market. The components of the gasoline are alkylate, ZSM-5 gasoline, and hydrocracker gasoline. The alkylate is of somewhat lower quality than alkylate produced from the conventional upgrading case due to dilution with C5 paraffins within the liquefaction plant. The ZSM-5 gasoline resembles cat cracker derived gasoline with a high octane rating, high olefins content, and moderate aromatics level. A lower yield loss is associated with the ZSM-5 upgrading compared to conventional catalytic reforming of the highly paraffinic F-T naphtha. The hydrocracker gasoline is of low quality and would be further upgraded in most petroleum refineries. It is the lowest octane material in either design case.

The diesel from the alternative upgrading case is identical to the hydrocracked component from the conventional case and has similar superior properties for diesel blending.

F-T PRODUCT VALUATION

The F-T derived materials were added to the blending pool of the midwest refinery model. After the introduction of these new blending stocks, the refinery configuration was re-optimized. Inclusion of these blending stocks resulted in reduced feedstock, operational, and capital costs. Thus, the F-T derived material was found to be more valuable than the refinery gasoline or diesel products. For example, the zero sulfur content of the F-T derived materials enable the refinery to reduce petroleum hydrotreating requirements, resulting in reduced capital and operating costs.

The results of the product valuation are shown in Table 4 for both Scenario I and Scenario II. This table shows that the F-T derived gasolines always command a premium over F-T derived diesel. Conventional wisdom has been that F-T derived gasoline is of low quality and F-T diesel production is preferable to gasoline production. This study suggest that this conventional wisdom is wrong for the U.S. fuels market. There are two explanations for this result. First, the U.S. market is skewed toward the production of gasoline which commands a higher price than diesel. Second, after upgrading F-T gasoline blending stocks are high quality components for blending to meet the CAAA gasoline specifications.

The ramifications of the price differential between gasoline and diesel can be further illustrated by comparing the alternative upgrading case to the conventional case for Scenario I. While the F-T gasoline from the alternative case is of lower value due to its low octane rating, the composite values for the gasoline and diesel are much closer due to the higher gasoline-to-diesel ratio for the alternative upgrading case. For Scenario II, the composite value for the alternative upgrading case is actually higher. This is a result of both the higher gasoline-to-diesel ratio and the negative effect of the high aromatics content of the F-T gasoline from the conventional upgrading case.

Alkylate and reformate are premium gasoline blending components and contribute significantly to the F-T gasoline value. Because of aromatics restriction in the CAAA, the reformate value, however, decreases in Scenario II. The ZSM-5 gasoline also was found to be a superior blending component. In Scenario I, the low value of the gasoline from the alternative upgrading was primarily a result of the low octane of the hydrocracker gasoline. However, in Scenario II this gasoline commands a substantial premium over the refinery gasoline product because of its zero sulfur and low aromatics contents, which are more critical in this scenario.

The high cetane and zero sulfur content of the F-T diesel blending stock was not found to have a significant effect on its value, which was only slightly higher than the price used for low-sulfur, on-highway diesel. The CAAA force the refiner to invest heavily in hydrotreating capacity both for gasoline and diesel sulfur reduction. Much of the desulfurization derives from gas oil (cat cracker feed) hydrotreating aimed primarily at lowering the sulfur content of the gasoline and hydrocracking aimed at increasing the gasoline yield. Any severe distillate hydrotreating required has the added benefit of improving the distillate cetane index. For these reasons, the refinery did not receive much benefit from the superior F-T diesel properties.

The implications of the F-T product values given in Table 4 on the economics of indirect liquefaction are reported elsewhere[2].

CONCLUSIONS AND RECOMMENDATIONS

The results of this study indicate that F-T derived materials look attractive for blending with conventional petroleum derived stocks to produce CAAA mandated transportation fuels. F-T derived gasoline blending stocks benefit the refinery due to their high octane, low sulfur content, and low olefins content. The F-T diesel, while superior to its petroleum counterpart, does not show much benefit to the typical refinery. However, it does command the same price as low sulfur diesel fuel. Further work is required to quantify the value of the high-cetane F-T diesel. Refinery specific situations might result in enhanced value for this material.

For Scenario I, the liquids from the conventional upgrading of the F-T product were more valuable than those from the alternative upgrading. This was reversed in Scenario II. Optimization of the F-T upgrading could improve the value of the gasoline from the alternative upgrading case. Octane improvement could possibly be achieved either by more severe ZSM-5 operation or by additional upgrading of the hydrocracker gasoline. Octane improvement for the conventional upgrading case is limited by the aromatics content of the reformate stream.

In addition, the alternative upgrading case results demonstrate the benefits of higher gasoline production from F-T upgrading. Other avenues for increasing the gasoline-to-diesel ratio from F-T upgrading include cat cracking F-T wax and low-wax F-T reactor operation. Both of these routes also could be used for the production of ethers for gasoline blending. Isobutylene and isoamylene can be converted directly to MTBE and TAME, whereas normal olefins must be converted to their iso-counterparts first. Skeletal isomerization could prove attractive for converting the large quantity of normal olefins obtained from iron-based F-T synthesis into etherification feedstocks.

Further work is necessary to optimize the production of transportation fuels from F-T synthesis. In addition to expanded LP studies including more upgrading options, experimental data are required to fill gaps in the existing LP data base and to confirm predictions from the LP model. Tests are necessary to establish the blending properties of the F-T derived materials. Additional testing of the ZSM-5 process for upgrading F-T liquids also should be performed.

The DOE-sponsored **Refining and End Use Study of Coal Liquids** will attempt to address some of the issues outlined above. Participants in this recently initiated project include Bechtel, Southwest Research Institute, Amoco, and M.W. Kellogg. Results from the present study indicate that Fischer-Tropsch synthesis could be an important technology for satisfying our nation's transportation fuel needs in the next century. The potential benefits of F-T derived fuels for meeting the environmental requirements of the CAAA have been quantified. More new insights are anticipated from the End Use Study.

REFERENCES

1) Choi, G.N., S.S. Tam, J.M. Fox, S.J. Kramer, J.J. Marano, "Baseline Design/Economics for Advanced Fischer-Tropsch Technology," **Proceedings of The Coal Liquefaction and Gas Conversion Contractors Review Conference**, September 27-29, 1993.
2) Choi, G.N., S.S. Tam, J.M. Fox, S.J. Kramer, J.J. Marano "Process Simulation for Indirect Coal Liquefaction Using Slurry Reactor Fischer-Tropsch Technology," **Symposium on Alternative Routes for The Production of Fuels**, ACS National Meeting, Washington, D.C., August 21-26, 1994
3) Kuo, J.C., et al. (Mobil), **Two-Stage Process for Conversion of Synthesis Gas to High Quality Transportation Fuels, Final Report**, DOE Contract No. DE-AC22-83PC60019, October 1985.

TABLE 1: CAAA 1990 Fuel Specifications

Gasoline Pool*:	Conventional	Scenario I Reformulated (Fed. Phase I)	Scenario II Reformulated (CARB Phase II)
% Reformulated		15 %	70 %
Summer RVP, psi	8.7 max	7.1 max	7.1 max
90% Point, °F	330 max	330 max	300 max
Sulfur, ppm	339 max	339 max	30 max
Olefins, LV%	9.2 max	9.2 max	4 max
Aromatics, LV%	32 max	26.2 max	22 max
Benzene, LV%	1.5 max	0.95 max	0.8 max
Oxygen, Wt%	-	2.1 min	2.1 min
Diesel Pool:			
% Low Sulfur		83 %	83 %
Sulfur, Wt%	0.25 max	0.05 max	0.05 max
Cetane Index	40 min	40 min	48 min

*The gasoline pool was assumed to be 42% premium grade (92 octane) and 58% regular grade (87 octane) in 2000.

TABLE 2: Typical Midwest Refinery Capacity and Production
(BPSD unless otherwise noted)

Unit Capacity:	1990	2000
Atmospheric Distillation	150,000	unchanged
Vacuum Distillation	59,300	unchanged
C5/C6 Isomerization	11,200	11,200-12,700
Naphtha Hydrotreating	45,900	unchanged
Catalytic Reforming	39,400	unchanged
Total Distillate Hydrotreating	21,300	31,200-34,200
Catalytic Cracking	53,300	unchanged
Hydrocracking	7,500	16,000-21,200
Delayed Coking	16,800	unchanged
Gas Oil Hydrotreating	-	27,600-28,300
C4 Isomerization	-	2,700-8,800
IC4 Dehydrogenation	-	0-4,100
MTBE/TAME Production	-	1,400-6,700
Alkylation	11,900	unchanged
Hydrogen Production, MMSCFD	7	31-39
Sulfur Production, LT/D	120	195-201
Production:		
LPG	4,270	4,270
Total Gasoline	72,730	78,760
Jet Fuel	12,500	14,680
Conventional Diesel	29,130	5,410
Low Sulfur Diesel	-	33,610
Residual Fuel/Asphalt	9,560	8,560

TABLE 3: F-T Derived Gasoline and Diesel Quality

Gasoline Pool:	Conventional* Upgrading	Alternate** Upgrading
Road Octane No.	88.4	81.1
RVP, psi.	5.1	6.0
90% Point, °F	294	305
Sulfur, ppm	0	0
Olefins, LV%	0	6.3
Aromatics, LV%	23.2	13.0
Benzene, LV%	0.2	0.5
Oxygen, Wt%	0.0	0.0
Diesel Pool:		
Sulfur, Wt%	0	0
Cetane Index	74.1	73.1

*Gasoline Pool: 37% alkylate, 23% isomerate, 40% reformate;
Diesel Pool: 67% hydrocrackate, 33% distillate;
Gasoline-to-Diesel Ratio: 0.97.

**Gasoline Pool: 35% alkylate, 36% ZSM-5 gasoline, 29% hydrocrackate;
Diesel Pool: 100% hydrocrackate;
Gasoline-to-Diesel Ratio: 1.8.

Table 4: Fischer-Tropsch Product Values
(dollars per barrel)

Crude Oil & Refinery Products:	Scenario I	Scenario II
Crude Oil	18.00	18.00
Composite Gasoline	26.00	26.70
Conventional Diesel Fuel	22.70	22.70
Low Sufur Diesel Fuel	24.80	24.80
F-T Conventional Upgrading:		
F-T Gasoline Blendstocks	27.02	28.07
F-T Diesel Blendstock	24.90	25.19
Composite for Conv. Upgrading	25.95	26.61
F-T Alternative Upgrading:		
F-T Gasoline Blendstocks	25.62	28.17
F-T Diesel Blendstock	24.91	25.19
Composite for Alt. Upgrading	25.36	27.10

PROCESS SIMULATION MODEL FOR INDIRECT COAL LIQUEFACTION USING SLURRY REACTOR FISCHER-TROPSCH TECHNOLOGY

Gerald N. Choi and Samuel S. Tam
(Bechtel Corporation, P.O. Box 193965, San Francisco, CA 94119)
Joseph M. Fox (Consultant)
Sheldon J. Kramer (Amoco Oil Company)
Shelby Rogers (DOE - Pittsburgh Energy Technology Center)

Key words: Indirect Coal Liquefaction
Advanced Fischer-Tropsch Technology
Process Simulation Model

INTRODUCTION

A detailed baseline design for indirect coal liquefaction using advanced Fischer-Tropsch (F-T) technology has been developed for Illinois No. 6 coal. This design forms the basis for an ASPEN process flowsheet simulation (PFS) model which can simulate the entire liquefaction plant and predict the effects of key process variables on the overall plant performance. A linear programming (LP) model based on a typical PADD II refinery was developed for product valuation and a discounted cash flow (DCF) spreadsheet model was developed for economic analysis. These closely coupled models constitute a research tool which the DOE can use to plan, guide and evaluate its ongoing and future research programs for the manufacture of synthetic liquid fuels by indirect coal liquefaction.

This paper covers the use of the ASPEN process simulation model and DCF spreadsheet model to look at the sensitivity of the economics to certain global process variables such as coal feed rate, synthesis gas conversion per pass and wax yield, together with certain specific reactor operating variables such as temperature, superficial velocity, slurry concentration, catalyst activity and catalyst life. Results are reported in terms of investment cost, yields and operating costs, which are then combined to determine a crude oil equivalent (COE) price. The COE is a hypothetical breakeven crude oil price at which a typical PADD II refinery could buy either crude oil or the coal liquefaction products. It is a present day value and is defined assuming constant deltas between crude oil and its products (i.e. constant refinery processing costs and margins).

OVERALL PLANT DESIGN

Block Flow Diagram

Figure 1 is a block flow diagram showing the overall process configuration. The facility is divided into three main sections:

1. Syngas production. Synthesis gas is generated in Shell gasifiers from ground, dried coal. Processing of the raw synthesis gas from the gasifiers is conventional, with wet scrubbing followed by single stage COS/HCN Hydrolysis and Cooling, Acid Gas Removal by inhibited amine solution and Sulfur Polishing. Sour Water Stripping and Sulfur Recovery units are included in this section.

2. The Fischer-Tropsch synthesis loop. The synthesis loop includes F-T Synthesis, CO_2 Removal, Recycle Gas Compression/Dehydration, Hydrocarbon Recovery by deep refrigeration, Hydrogen Recovery and Autothermal Reforming. The Hydrocarbon Recovery Unit also includes deethanization, depentenization, fractionation and an oxygenates wash column. At low H_2/CO ratios, CO_2 is the primary byproduct of the F-T reaction so a large CO_2 removal unit is required. In the Autothermal Reformer, unrecovered light hydrocarbons in the recycle gas are converted to additional syngas which raises the H_2/CO ratio to the F-T reactors.

3. Product upgrading. The downstream upgrading units include Wax Hydrocracking, Distillate and Naphtha Hydrotreating for oxygenate removal and olefin saturation, Catalytic Naphtha Reforming, C_4 Isomerization, once-through C_5/C_6 Isomerization, $C_3/C_4/C_5$ Alkylation and a Saturate Gas Plant. Liquid wax from the reactor, after catalyst recovery, is sent to the hydrocracker where high quality distillates are produced along with some naphtha and light ends. The naphtha, along with hydrotreated F-T naphtha, is catalytically reformed into aromatic gasoline blending components. Light hydrocarbons are isomerized and alkylated into quality gasoline blending stocks.

The F-T slurry reactor is essentially a bubble column reactor where the slurry phase is a mixture of molten wax and catalyst. The gas provides the agitation necessary for good mixing and mass

transfer of reactants to, and products from, the liquid phase. The slurry reactor was chosen over the fixed-bed reactor for the Fischer-Tropsch section based on an earlier Bechtel study[1,2].

Further details concerning the design basis, process selection, cost estimating procedures and alternative cases studied are given in a paper presented at the 1993 DOE/Coal Liquefaction and Gas Conversion Contractors Review Conference[3].

Product and Byproduct Yields

The F-T liquefaction facility produces C_3 LPG, an upgraded C_5 - 350 °F naphtha and 350 °F - 850 °F combined light and heavy distillates. The primary byproduct is liquid sulfur. Yields and product qualities, along with the baseline design F-T reactor operating conditions are given in Table 1. The hydrocarbon products have no measurable sulfur or nitrogen contents because of the requirements and nature of the Fischer-Tropsch reaction. Oxygen is removed to less than 30 ppmv. There are virtually no aromatics in the distillate. Olefins are saturated to low levels of residual olefin concentration in both the naphtha and the distillate. The diesel fraction has a very high cetane number, on the order of 70, and the jet fuel fraction and heavy distillates have low smoke points.

The naphtha product is a mixture of $C_3/C_4/C_5$ alkylate, C_5/C_6 isomerate and catalytic reformate. It is basically a raw gasoline with a clear (R+M)/2 octane number of about 88. If insufficient butanes are available to alkylate all of the available C3/C4/C5 olefins, then n-butane is purchased and isomerized.

PROCESS SIMULATION MODEL

The process flowsheet simulation model predicts the effects of key process variables on the overall material and utility balances, operating requirements and capital costs. This model is implemented in the PC version of ASPEN/SP.

Development of the Model

Baseline design information was transmitted from Bechtel to Amoco for the development of the process flowsheet simulation computer model. Information transfer was expedited by Bechtel's development of a preliminary ASPEN/SP model for the design of the F-T synthesis loop. The computerized F-T slurry reactor yield correlations used for design purposes have been discussed previously[4].

The computer model was developed as a planning/research guidance tool for the DOE and its subcontractors. The model is not designed to be a plant design and sizing program for every plant in the complex. The F-T synthesis loop design is handled in some detail and Bechtel's F-T reactor sizing and yield models are built into the design. For other plants, only overall yield, utility requirements and capital costs are estimated. Costs are prorated on capacity using cost-capacity exponents and information on the maximum and minimum capacity of single train plants.

All ISBL plants in the three main processing sections discussed earlier are simulated; some by a combination of ASPEN/SP process simulation blocks and user Fortran blocks and some by just user Fortran blocks. Material balances, as well as utility consumptions, operating personnel requirements and ISBL costs for each plant are produced. The OSBL, engineering and contingency costs are estimated from the ISBL plant costs to generate the total installed cost of the facility.

This ASPEN model generates a file for direct transfer of the significant model results to the DCF spreadsheet economics model. The spreadsheet model takes this input, and with a given set of financial assumptions calculates the cost of production and a crude oil equivalent price for a 15% return on investment.

F-T product values were generated by a linear programming model of a typical PADD II refinery at present day crude oil prices. These results are being reported separately at this meeting[5]. In calculating the COE, several different assumptions can be used to relate feed and product values to crude oil price. The DCF spreadsheet allows for the use of a constant value, a constant ratio or a constant delta. Since what is desired is the equivalent refinery processing cost to produce the same product, this paper uses a constant delta to relate the hydrocarbon products and imported butane prices to the crude oil price. The effect of varying these deltas is shown.

Caution should be used in extrapolating COE to future pricing scenarios and drawing conclusions as to when coal liquids will become competitive with equivalent products from crude oil. The COE, as herein defined, is a conceptual tool allowing various yield configurations and coal processing scenarios to be compared as a single number on the basis of present day

economics. When future projections are made, it is necessary to consider inflation in construction costs as well as various price escalation scenarios for crude oil, coal and other energy sources. Such studies are beyond the scope of this paper.

PROCESS SENSITIVITY STUDIES

The PFS model is designed to handle the effects of the following process variables:

Primary Variables	Range
Coal Feed Rate	4,500 to 45,000 mtpd
F-T Conversion per Pass	50 to 82%
F-T Wax Yield	10 to 75%
F-T Reactor Inlet Superficial Velocity	5 to 20 cm/s
F-T Reactor Catalyst Concentration	20 to 40%
Secondary Variables	
H_2/CO Ratio	0.36 to 0.7
Heat Transfer Flux	68,000 KJ/hr-m^2 - 114,000 KJ/hr-m^2 (6,000 - 10,000 Btu/hr-ft^2)
Flow Regime	Bubble to Churn Turbulent

Baseline design conditions are 18,400 mtpd coal feed rate, 82% conversion, 50% wax yield, 10 cm/s superficial velocity and 22.5 wt% slurry.

This paper presents the results of parametric economic studies covering the primary variables cited above. A brief summary follows:

Effect of Design Plant Capacity - The effect of plant capacity on the overall F-T facility capital investment is exponential with an average cost-capacity exponent of 0.89. This large an exponent is not surprising since multiple process trains are involved. The effect on COE, over the entire range, is about $0.80/bbl.

Effect of Design F-T Syngas Conversion Per Pass - As expected, high conversion per pass is economically favorable. Decreasing the syngas conversion from 82 to 68% at a constant 18,400 mtpd coal feed rate increases total plant investment by approximately 9%, with the main effect being on the F-T synthesis section loop due to increased recycle. The L/D of the F-T reactor becomes much smaller at low conversion and the designs become impractical unless other parameters, such as slurry concentration, are relaxed as well.

Effect of Design Wax Yield - The effect of design wax yield at the baseline capacity of 18,400 mtpd coal feed rate was studied over the range of 10 to 75 wt%, obtained by varying F-T reactor temperature from 271 to 242 °C. Increasing the wax yield from 10 to 75 wt% reduces the F-T naphtha to distillates production ratio from 2.38 to 0.62. An increase in light olefins production at 10 wt% wax yield requires the purchase of roughly 11,000 bbl/day of butane to make alkylate, whereas the 75 wt% wax yield case is in butane balance.

The F-T reactor size becomes larger at high wax yield and there is a minimum in plant investment cost at about 50 wt% wax yield. The variation in total plant cost, over the entire range of wax yields, is less than 3%. The optimum wax yield is highly dependent on the price of purchased butane, gasoline and diesel relative to crude oil. Present day price spreads for F-T gasoline and distillates relative to crude oil were determined as $9.00/bbl and $6.90/bbl, respectively, by linear programming studies[5]. The present price for butane is $3.50/bbl. less than crude oil. Using these deltas, the optimum wax yield appears to fall between 50 to 60 wt%.

Lowering the butanes price relative to crude oil drastically alters this trend, and when butanes are priced at $20/bbl under the price of crude oil, the low wax yield case is preferred. The linear programming studies did not credit the exceptionally high cetane number of the F-T distillate product. Other sources indicate that a delta of $9.0/bbl instead of $6.90/bbl for the F-T distillates may be more realistic and this lowers the COE by $1.00 per barrel and makes the optimum wax yield slightly higher.

Effect of Slurry F-T Reactor Design Variables - The inlet superficial gas velocity was studied in conjunction with slurry concentration. The reason is that, if varied independently, as soon as these variable depart from the baseline design, the reactor L/D changes. Increasing superficial velocity, at constant slurry concentration, leads to impractically high L/D ratios for which the costing algorithm is not equipped to handle accurately. This can be compensated for by increasing slurry concentration. Figure 2 shows the combination of superficial velocity and slurry concentration necessary to maintain a constant L/D of 3.15 (the baseline design reactor). The reactor inside diameter has been kept between 3.8 to 5.0 meters (12.5 to 16.5

feet) by varying the number of reactors from 48 to 16. The baseline design, at 10cm/s superficial velocity and 22.5 wt% slurry concentration, has eight F-T synthesis trains with 3 reactors per train, each reactor being 5 meters ID by 15.8 meters T-T.

Figure 2 also shows the total cost of reactors as a function of the superficial velocity and slurry concentration while maintaining a constant reactor L/D of 3.15. The cost is inversely proportional to the inlet superficial gas velocity. The potential savings on increasing the superficial gas velocity from 5 to 20 cm/s is on the order of $80 million, and this results in a reduction of the COE by about $0.80/bbl.

CONCLUSIONS AND RECOMMENDATIONS

These preliminary parametric sensitivity studies demonstrate the capability of the process flowsheet simulation model. When coupled to a discounted cash flow spreadsheet model, its effectiveness for examining the effects of various process variables on the F-T indirect coal liquefaction costs and economics has been demonstrated. The responsiveness of the model to a variety of F-T slurry reactor operating conditions has also been established.

REFERENCES

1) Fox, J.M.. "Slurry vs. Fixed-Bed Reactors for Fischer-Tropsch and Methanol", 1990 Topical Report - DOE Contract No. DE-AC22-89PC89876.

2) Fox, J.M., "Fischer-Tropsch Reactor Selection", Catalysis Letters 7 (1990) 281-292

3) Choi, G.N., Tam, S.S., Fox, J.M., Kramer, S.J. and Marano, J.J. "Baseline Design/Economics for Advanced Fischer-Tropsch Technology", DOE/Proceedings of The Coal Liquefaction and Gas Conversion Contractors Review Conference, September 27-29, 1993.

4) Fox, J.M. and Tam, S.S. "Correlation of Slurry Reactor Fischer-Tropsch Yield Data", Symposium on Fischer-Tropsch and Alcohol-Synthesis, ACS 1994 Spring Meeting, San Diego, California, March 14-18, 1994.

5) Marano, J.J., Rogers, S., Choi, G.N. and Kramer, S.J., "Product Valuation of Fischer-Tropsch Derived Fuels", Symposium on Alternative Routes for The Production of Fuels, ACS National Meeting, Washington, D.C., August 21-26, 1994.

Table 1
Baseline Facility Design

Feed:	
ROM as received coal	7.68×10^5 Kg/hr (18,420 mtpd)
N-Butane	1.20×10^4 Kg/hr (3,120 BPSD)
Electric power	50 MWh
Primary Products:	
C3 LPG	6.45×10^3 Kg/hr (1,920 BPSD)
F-T gasoline blend	1.14×10^5 Kg/hr (23,900 BPSD)
F-T diesel blend	1.26×10^5 Kg/hr (24,700 BPSD)
Sulfur	2.12×10^4 Kg/hr
F-T Operating Conditions:	
Temperature/pressure	253 °C/2.17 MPa (50% wax)
Syngas conversion	81.7 %
Inlet superficial gas velocity	10.0 cm/sec
Catalyst slurry concentration	22.5 wt%
Catalyst make-up rate	0.5 % per day

mtpd [=] metric tons per stream day
BPSD [=] Barrels per stream day

Figure 1
INDIRECT COAL LIQUEFACTION BASELINE STUDY
OVERALL PROCESS CONFIGURATION

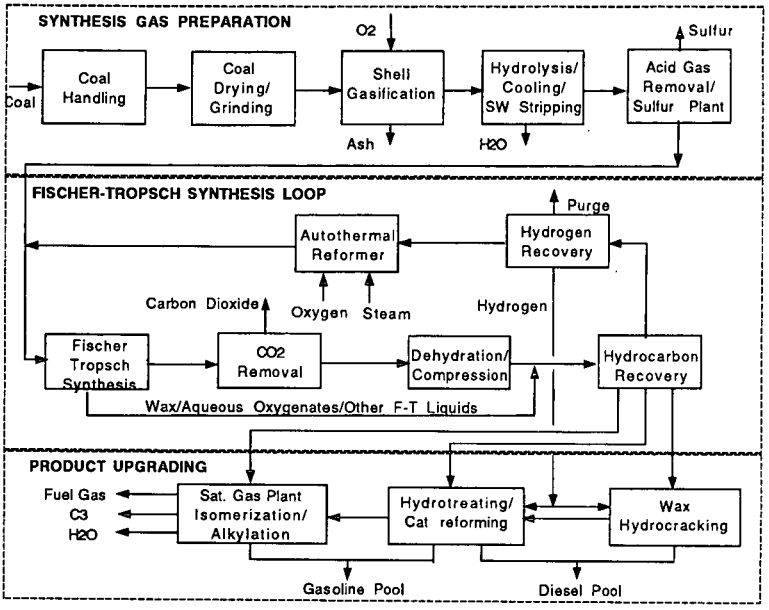

Figure 2
Total F-T Reactor Cost at Constant L/D of 3.15

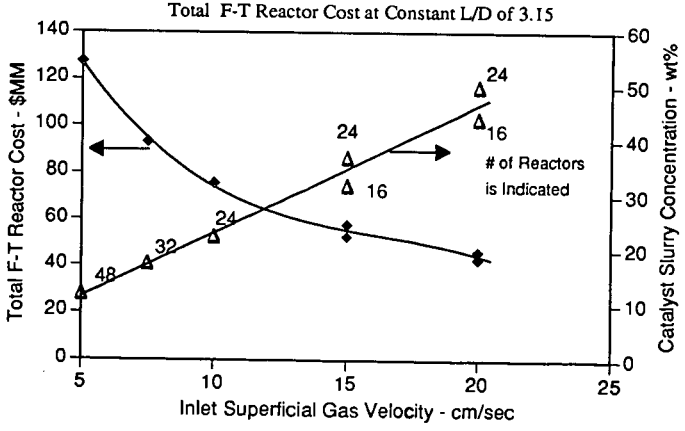

COPRODUCTION OF HYDROGEN AND ELECTRICITY : CATALYTIC APPLICATIONS

G. Alex Mills
Center for Catalytic Science and Technology
Department of Chemical Engineering, Newark, DE 19716

Keywords: Hydrogen; Electricity; Catalysis.

There is a growing need for new technology for more economical manufacture of hydrogen and for generation of electricity, dictated by increasingly stringent environmental requirements.

Environmentally benign transportation fuels almost always require hydrogen for their manufacture. Hydrogen is needed for production of high-performance oxygenate fuels - alcohols and ethers. Hydrogen is needed for hydrodesulfurization. Also, it is expected that hydrogen will be needed for conversion of aromatics to naphthenes to meet environmental requirements. There is a growing recognition that there will be a significant future shortage of hydrogen supply.

The electric utility industry is most affected by the 1990 Clean Air Act Amendments requirements for the reduction of SO_2 and NO_x to meet acid rain provisions (Title IV) and by control of NO_x in ozone nonattainment areas (Title I). The CAAA requires reduction of SO_2 to half of 1980 levels.

These needs provide the motivation for the present paper which examines catalytic opportunities for advantageous *coproduction* of hydrogen and electricity from coal, peroleum coke and/or biomass. The strategic concept involves modifications of the Integrated Gasification - Combined Cycle process. In IGCC, coal, petroleum coke or biomass is converted to synthesis gas, a mixture of H_2, CO and CO_2. This syngas is used as fuel for generation of electricity in a combined turbine and steam cycle. The IGCC plant process steps of **gasification**, **gas purification**, and **gas turbine** and **steam cycle** for production of electricity are illustrated in Fig.1. Including the Cool Water plant in California, four IGCC coal-based demonstration plants have been built and operated world-wide. Eight additional plants are in various state of development under the DOE Clean Coal Program. A 305MWe plant is under construction in Spain. IGCC plants based on petroleum coke are in advanced planning and commitment stages.

It has been proposed that the IGCC process be modified so that part of the synthesis gas is converted to chemicals and then the remainder of the syngas is used to generate electricity. Such a plant has been termed a powerplex. Technology for coproduction of electricity and methanol and dimethyl ether, (including once-through catalytic slurry-phase operation) have been proposed, and syngas conversion tested experimentally under appropriate conditions (1). The economics of oxygenates / electricity cogeneration evaluated and deemed to be favorable under certain conditions (2).

In this paper, various technologies for coproduction of hydrogen and electicity are proposed. Possible advantages are: pollution abatement; higher efficiency; and improved economics; and use of national resources of coal, petroleum coke and biomass. Emphasis is given to eight potential catalytic process applications, indicated in Fig. 1.

1 Catalytic Gasification. Gasification of solid fuels is carried out in the presence of steam by partial combustion at 900° - 1500° C. It has long been known that alkali hastens the critical slow reaction, $C + H_2O \rightarrow CO + H_2$. Extensive laboratory and pilot plant studies have established reaction mechanisms and practical process information (3). It was demonstrated that catalytic gasification of coal can be carried out at industrial rates at 600 - 700 °C. (3, 4).

2 Integral Catalytic Gasification / Synthesis ICG/S is the concept of carrying out integral, that is simultaneous, gasification and synthesis of desired fuel hydrocarbons or oxygenates. Gasification and synthesis of methane was first proposed. Fairly high yields of CH_4 becomes thermodynamically stable in the presence of steam and carbon at 700°C and higher pressures, Fig. 2 (5). Indeed, potassium is also a catalyst for methane formation and high methane levels were found in extensive catalytic coal gasification pilot plant operations carried out at Exxon with DOE support (3,4) This process has not been commercialized.

It is now suggested that a combination of gasification and oxygenate-synthesis catalysts be utilized to accomplish gasification and oxyenates synthesis. A problem is matching rates of gasification and thermodynamic contraints of oxgenate synthesis. at a common temperature and pressure. Synthesis of methanol is carried out at about 300° C. One option to increase synthesis conversion is to operate so as to produce methanol and dimethyl ether. Higher yields of MeOH and DME are thermodynamically possible at a fixed temperture/pressure conditons than for

methanol alone (6). Another option is gasification / production of mixed, higher alcohols. Higher alcohols, including isobutyl alcohol, were manufactured at temperatures as high as 500 °C. Production of hydrogen from oxygenates is discussed later.

3 Catalytic Water Gas Shift The composition of synthesis gas is sensitive to gasification conditions, including the presence of larger amounts of steam, used in the Texaco process. Another application of catalysis is the adjustment of gas composition to that most suitable for further synthesis processing. The catalytic water gas shift processes high, 350° C, and low, 200° C, are well established industrially for hydrogen manufacture by the reaction, $CO + H_2O \rightarrow CO_2 + H_2$. Incorporation of the WGS reaction presents useful options in synthesis process technologies now discussed.

4. Catalytic Oxygenates Synthesis.
Higher alcohols synthesis also offers opportunities for production of valuable coproducts, perhaps particularly isobutanol which has potential high value as an octane-enhancing gasoline additive. Several opportunities for improved higher alcohols synthtsis has recently been presented.7)

5 Catalytic Reforming of Oxygenates for Hydrogen Manufacture.
A problem in coproduction of hydrogen and electricity is flucuating electricity demand which results in variable hydrogen generation rates. Gaseous hydrogen is not easily stored. If more easily-stored liquid methanol and dimethyl ether are produced, they can be utilized for production of hydrogen by catalytic decomposition or by catalytic steam reforming. Technology for reforming oxygenates for production of hydrogen is well established, has been used in certain instances, and may be a useful option component in an energyplex. Methanol decomposition is used for production of supplemental fuel gas in Berlin for peak demand conditions

The conversion of methanol (and DME) to syngas is endothermic. The synthesis gas formed has higher heat of combustion than the methanol from which it is produced. It has been proposed that when *waste heat* is used to supply endothermic energy required for syngas formation, there would be an effective increase in heat value of the methanol, for automotive or electrical generation applications. Endothermic dissociation $CH_3OH(g) \rightarrow 2H_2 + CO$, $\Delta H_{298K} = 21{,}664$ cal/g-mole. Including the heating value increase in the methanol vaporization step, endothermic dissociation can increase the fuel heating value by over 20% over liquid methanol (8). If hydrogen is the sole desired fuel, methanol can be steam reformed. $CH_3OH(g) + H_2O \rightarrow 3H_2 + CO_2$, $\Delta H_{298K} = 11{,}826$ cal/g-mole. Including the heating value gained from methanol vaporization, the reformed methanol can have about 13% higher heating value than liquid methanol (8)

6 Electrocatalytic Hydrogen Separation.
A new technique for hydrogen separation is an outgrowth of fuel cell technology. An electrochemical cell is used which has highly efficient catalytic electrodes. Impure hydrogen is consumed at the anode of the cell and purified hydrogen generated at the cathode, Fig 3. By the application of a small potential across the electodes of this cell, it is possible to ionize H_2 at the anode and simultaneously to produce an equivalent amount of high purity H_2 at the cathode. The effect of gaseous feed rate over an anode on hydrogen removal efficiency is illustrated in Fig. 4 showing data from an early publications from the Houdry Laboratory (9, 10) .This concept has been much further developed with promising results. It has been shown that 80% of hydrogen recovery is feasible from very dilute H_2-containing streams, Fig 5 (11) It is a critical point that the catalytic electrodes are very efficient (low overvoltage). Therefore, only a small amount of electricity is required, namely 2to 10 kw-hr per 1000 ft^3 of hydrogen. In the present application hydrogen not separated is not wasted but is utilized as fuel in the combined cycle generation of electriciy.

7 Catalytic Fuel Cells. Fuel cells are catalytic devices. It should also be pointed out that a fuel cell could be used advantageously to supply the needed electricity for the electrocatalytic hydrogen separation, utilizing a small part of the hydrogen produced. Fuel cells are not discussed further here except to note that they could be used instead of or in combination with combined cycle for electicity generation

8 Membrane Separation, Separation/ Catalysis.
Membranes offer special opportunities for separation of hydrogen from gaseous mixtures, based on diffusion, on sieving, or on permeation. The commercial Monsanto PRISM process utilizes hollow fiber membranes with an active siloxane layer. Active research is underway to develop membranes capable of separating gas mixtures based on molecular size, using molecular sieving mechanism. One direction is to begin with a mesoporous membrane (> 50A) and to apply a layer of an inorganic oxides such as silica to produce a microporous structure.(12). A gas separation membrane multi-layer structure has been described (13). Another approach is to utilize carbon molecular sieve and to reduce the pore size to 3 or 4 A, evaluated for separation of CO_2 and H_2 (14)

It is also possible to utilize a metal membrane. A special membrane is palladium which has almost infinite selectivity for passage of hydrogen. Here the mechanism is conversion to a hydride, migration of the hydride and reformation of molecular hydrogen. Palladium membrane have been used commercially for hydrogen purification. Pd alloyed with Ag or other metals has shown advantages (15). A metal-membrane-based process for production of hydrogen is based on a novel hydrogen-permeable composite membrane. Separation by permeation is also possible.

Combining separation and catalysis offers much potential. By removal of a reaction product for a thermodynamically limited reaction, the reaction can be driven further, as in the water gas reaction (16). Other reactions which could be combined are hydrodesulfurization or other hydrogenation reactions such as of aromatics to naphthenes.

Pressure Swing Adsorption Pressure Swing Adsorption, not a catalytic process, is used for separation in modern plants for manufacture of hydrogen.Microporous solids are used, in many ways structurally similar to catalysts. PSA offers a bench mark for comparison with alternative separation processes.

In summary, attention is drawn to a number of catalytic options which are deemed promising for needed new technology for production of hydrogen and electricity, technology which will be environmentally advantageous (16). Further, it is suggested that the electrical industry will be involved with catalytic chemistry and engineering.

References

1. Brown, D.M., Henderson, J.L., Hsiung, T.H., Studer, D.W. EPRI 15th Annual Conference on Fuel Science and Conversion. Palo Alto, CA June (1990).
2. Houston Light & Power Co. EPRI report TR-101789 Project 3226-04, (1992).
3. Penner, S., Wiesenhahn, D.F. *Energy,* Vol. 12, No. 8/9 pp 623-903, (1987).
4.Hirsch, R.L., Gallagher, J.E., Lesserd, R.R., Wesselhoft, R.D. Science vol.215, No. 4529 pp 121-127.(1982).
5. Haussinger, P., Lohmuller, R. Hydrogen. Ullman's Encyclopedia of Chemical Technology. VCH, (1989).
6. Hansen, J.B., Joensen, F. " High Conversion of Synthesis Gas to Oxygenates in Natural Gas Conversion." Natural Gas Conversion Symposium Proceedings. Eds A.Holman et al. Amsterdam. Elsevier, pp 457-467 (1991).
7. Summary of Higher Alcohols Synthesis Workshop. Ed, P. Zhou. DOE Contract DE-AC22-89PC88400 subtask 43.02 Feb. (1994)
8. Yoon, H., Stouffer, M.R., Dudt, P.J., Burke, F.P., Curran, G.P. Energy Progress 5: pp78-83, (1985).
9. McEvoy, J.E., Hess, R.A., Mills, G.A., Shalit, H. "Hydrogen Purification Using a Modified Fuel Cell Process". Ind. & Eng. Process Design and Development. Vol. 4, pp1-3,.(1965)
10. McEvoy, J.E, "Electrolytic Method of Gas Separation", U.S.Patent 3,401,099.(1968).
11. Farooque, M., Kush, A., Abens, S. Novel Electrochemical Hydrogen Separation Device Using Phosphoric Acid Membrane Cell. Separation Science and Technology. 25 (13-15^{9}) pp 1361-1373 (1990).
12. Gavalas, G.R. "Hydrogen Separation by Ceramic Membranes"'in Proceedings of the Twelfth Annual Gasification and Gas Stream Cleanup Systems Contractors Meeting, Johnson and Jain, Eds. DOE Morgantown, W.VA. pp 338-345 Sept. (1992).
13. Goldsmith, R.L., Higgins, R.J., Bishop, B.A. 'Low Cost Ceramic Membranes and Supports for Gas Separations' see ref (12) p205-217.(1992).
14. Yates, S.F., Swamikannu, A.X. High Temperature Size Selective Membranes. Proceedings of the Coal-Fired Power Systems 93 Advances in IGCC and PFBC Review Meeting,.D.L.Bronk, Ed, U.S. DOE, Morgantown, W,VA. DE93000289 June (1993).
15. Armor, J.N. "Challenges in Membrane Catalysis". Chemtech. Sept. 557-563.(1992)
16. Edlund, D.J. Catalytic Membranes Facilitating the Water Gas Shift Reaction see ref 14, pp 233-237 (1993)
17. Mills, G.A. Status and Future Opportunities for Conversion of Synthesis Gas to Liquid Energy Fuels D.O.E , NREL/TP 421-5150, NTIS 93010025.(1993).

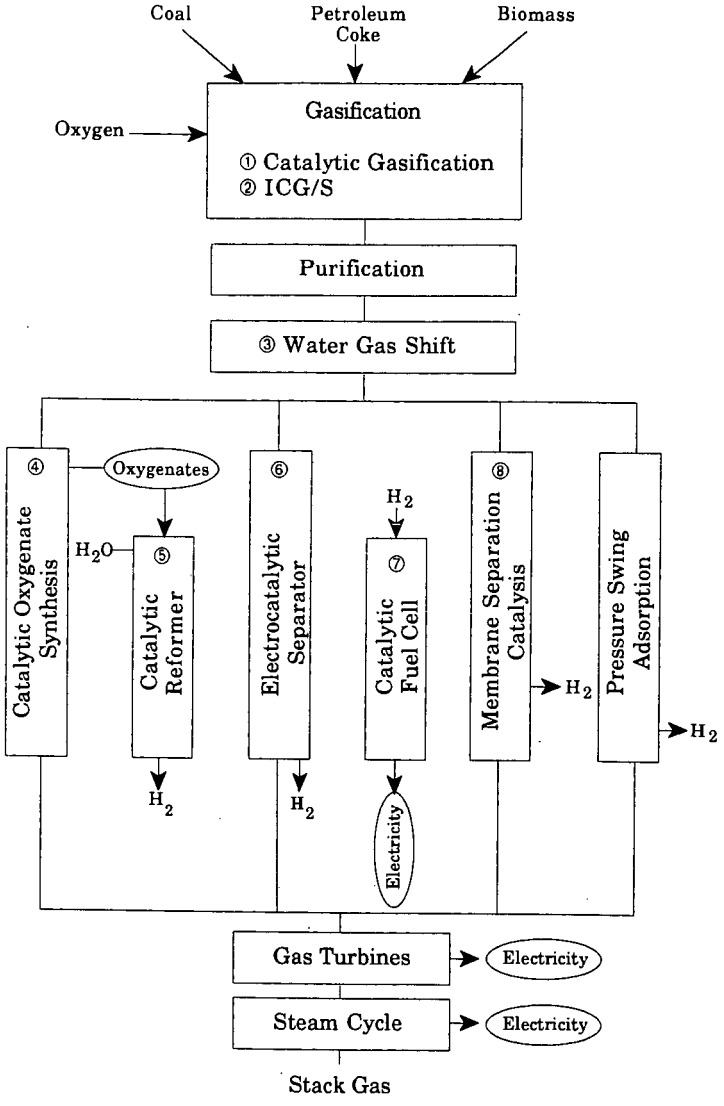

Fig. 1. Catalytic Modifications of IGCC for Production of Hydrogen and Electricity

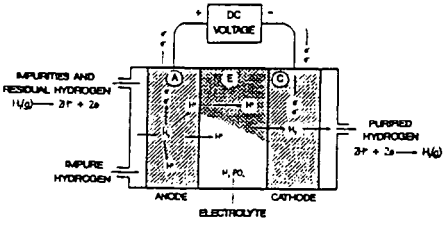

Fig. 3. Schematic of an electocatalytic hydrogen separator (11).

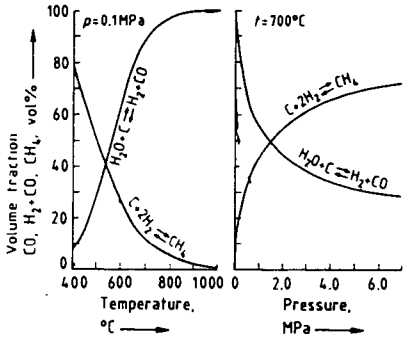

Fig. 2. Effect of temperature and pressure on equilibrium gas composition in the presence of carbon (5).

Hydrogen Removal Efficiency from 12% H_2 Stream

Plot No.	*Feed Rate, Cc./Min.*	*% Efficiency*
1	4.2	73.0
2	9.5	71.4
3	15.4	65.8

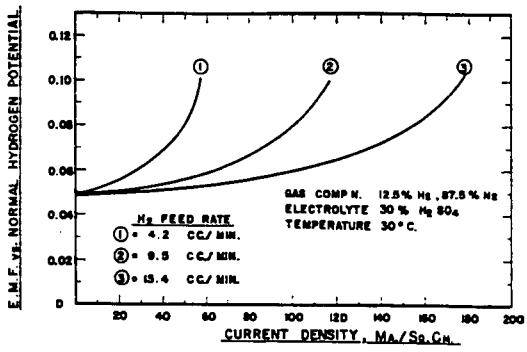

Fig. 4. Effect of feed rate on anode performance in electrocatalytic separation (9).

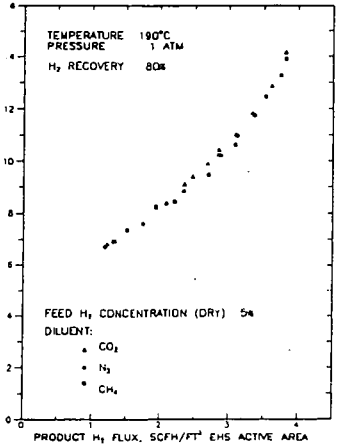

Fig. 5. Electrocatalytic Hydrogenation Separation performance with dilutants (11).

EQUILIBRIUM THERMODYNAMIC ANALYSIS OF LIQUID-PHASE ETHYL *TERT*-BUTYL ETHER (ETBE) SYNTHESIS

Kyle L. Jensen and Ravindra Datta*
Department of Chemical and Biochemical Engineering
The University of Iowa
Iowa City, Iowa 52242

Keywords: Reaction equilibrium, equilibrium constant, ethyl tert-butyl ether (ETBE)

INTRODUCTION

There are two forces driving the increasing usage of oxygenates (alcohols and ethers) in gasoline. First, lead compounds, long used for octane improvement in gasoline, have now been phased out by the EPA. The second reason is the Clean Air Act Amendments (CAAA) bill of 1990, which has two programs involving the use of oxygenates: 1) *Oxygenated Gasoline Program* that requires the use of gasoline containing a minimum of 2.7 wt. % oxygen in 44 cities during the four winter months as a strategy to reduce CO emissions; and 2) *Reformulated Gasoline Program* for the nine worst ozone non-attainment areas, beginning Jan 1, 1995, that will require gasoline reformulation to lower toxic and ozone generating pollutants (VOC emissions), but containing atleast 2 wt. % oxygen.

The main competing oxygenates at present, are ethanol and methyl *tertiary* butyl ether (MTBE, or 2-methoxy 2-methyl propane). MTBE is now the second largest volume organic chemical, only behind ethylene, produced in the U.S. (Reisch, 1994). This is remarkable since its commercial production began barely two decades ago. Although MTBE is currently the industry standard, it has been proposed (Lucht, 1993) that ethanol and other renewable additives make up to 30% of the oxygenate market. This proposal is aimed primarily at reducing dependence on the finite fossil fuel resources. Furthermore, it would alleviate concerns about the buildup of carbon dioxide in the atmosphere, the major "greenhouse" gas. As a result, ethyl *tertiary* butyl ether (ETBE, or 2-ethyoxy 2-methyl propane), derived from renewable ethanol and isobutylene, has emerged as a promising new oxygenate . ETBE also has a somewhat lower blending Reid vapor pressure as well as a higher octane number than MTBE.

The commercial production of ETBE, by the equilibrium limited exothermic reaction of ethanol and isobutylene over an acid ion exchange catalyst, has recently begun (Oxy-Fuel News, 1992). In spite of its anticipated industrial importance, reliable information on the thermodynamics of the liquid-phase formation of ETBE is virtually non-existent in the open literature. Iborra et al. (1989) proposed an expression for the equilibrium constant for the ETBE reaction in the *gas* phase. However, since commercially the reaction occurs in the liquid phase, it is the thermodynamics of the liquid-phase reaction that is of the principal interest. Vila et al. (1993) have recently reported an expression for the liquid-phase ETBE equilibrium constant; however, the constants of integration in it were used as fitted parameters. Consequently, a careful thermodynamic analysis is warranted, and is provided here along with experimental data over a range of temperatures of practical interest. Alternate thermodynamic pathways are considered by Jensen and Datta (1994).

THERMODYNAMIC EQUILIBRIUM CONSTANT

The equilibrium constant for the non-ideal liquid-phase reaction, $\sum_{j=1}^{n} \nu_j A_j = 0$, among the species A_j is

$$K(\ell) \equiv \prod_{j=1}^{n} a_{je}^{\nu_j} = \left(\prod_{j=1}^{n} \gamma_{je}^{\nu_j}\right)\left(\prod_{j=1}^{n} x_{je}^{\nu_j}\right) \equiv K_\gamma K_x \qquad (1)$$

The second equality stems from the definition of activity, $a_j \equiv \gamma_j x_j$. Upon relating the activity coefficients, γ_j, to the mole fraction, x_j, through an appropriate relation, such as the UNIFAC correlation, the equilibrium composition may be determined for a given $K(\ell)$. The equilibrium constant, in turn, is related to the thermodynamic properties of the mixture through

$$K(\alpha) = \exp\left\{-\frac{\Delta G_T^\circ(\alpha)}{RT}\right\} \qquad (2)$$

for a reaction occurring in a phase α at the reaction temperature T. The standard Gibbs energy change for the reaction

$$\Delta G^{\circ}_{T}(\alpha) = \sum_{j=1}^{n} \nu_j \, \Delta G^{\circ}_{fjT}(\alpha) \tag{3}$$

where $\Delta G^{\circ}_{fjT}(\alpha)$ is the Gibbs energy of formation of species j in the phase α at the reaction temperature, T. Alternatively, the standard Gibbs energy change for the reaction may be computed from the standard enthalpy and entropy change for the reaction at the temperature T by

$$\Delta G^{\circ}_{T}(\alpha) = \Delta H^{\circ}_{T}(\alpha) - T\Delta S^{\circ}_{T}(\alpha) \tag{4}$$

where the change in the standard enthalpy and entropy are determined by equations of the form of eq 3 for the reaction fin the α phase.

Normally the reported data on Gibbs energy and enthalpy of formation are, however, available only at the standard state (ideal gas; $P^{\circ} = 1$ bar; $T^{\circ} = 298.15$ K), rather than at the reaction conditions of interest (e.g., condensed phase; $P \neq P^{\circ}, T \neq T^{\circ}$). While the effect of pressure is usually small, $\Delta G^{\circ}_{T}(\alpha)$ for temperatures and phase other than the standard is obtained as follows. Using an integrated form of the v'ant Hoff equation the effect of temperature may be accounted for by

$$\frac{\Delta G^{\circ}_{T}(\alpha)}{RT} = \frac{\Delta G^{\circ}_{T^{\circ}}(\alpha)}{RT^{\circ}} - \frac{1}{R}\int_{T^{\circ}}^{T} \frac{\Delta H^{\circ}_{T}(\alpha)}{T^2}\, dT \tag{5}$$

where the enthalpy of reaction as a function of temperature may be obtained from the Kirchoff equation

$$\Delta H^{\circ}_{T}(\alpha) = \Delta H^{\circ}_{T^{\circ}}(\alpha) + \int_{T^{\circ}}^{T} \Delta C^{\circ}_{P}(\alpha)\, dT \tag{6}$$

where for the reaction

$$\Delta C^{\circ}_{P}(\alpha) \equiv \sum_{j=1}^{n} \nu_j \, \Delta C^{\circ}_{Pj}(\alpha) \tag{7}$$

The molar heat capacities of species are generally expressed as a polynomial in temperature of the form (Reid et al., 1987)

$$C^{\circ}_{Pj}(\alpha) = a_j(\alpha) + b_j(\alpha)T + c_j(\alpha)T^2 + d_j(\alpha)T^3 \tag{8}$$

Upon using eqs 7 and 8 and carrying out the integration in eq 6, there results

$$\Delta H^{\circ}_{T}(\alpha) = I_H(\alpha) + \Delta a(\alpha)T + \frac{\Delta b(\alpha)}{2}T^2 + \frac{\Delta c(\alpha)}{3}T^3 + \frac{\Delta d(\alpha)}{4}T^4 \tag{9}$$

where $I_H(\alpha)$ is the constant of integration obtainable from Eq 9 by using $T = T^{\circ}$ and

$$\Delta a(\alpha) \equiv \sum_{j=1}^{n} \nu_j a_j(\alpha) \; ; \; \Delta b(\alpha) \equiv \sum_{j=1}^{n} \nu_j \, b_j(\alpha)$$
$$\Delta c(\alpha) \equiv \sum_{j=1}^{n} \nu_j \, c_j(\alpha) \; ; \; \Delta d(\alpha) \equiv \sum_{j=1}^{n} \nu_j \, d_j(\alpha) \tag{10}$$

The use of eq 9 in eq 5 results in

$$\frac{\Delta G^{\circ}_{T}(\alpha)}{RT} = -I_K(\alpha) + \frac{I_H(\alpha)}{RT} - \frac{\Delta a(\alpha)}{R}\ln T - \frac{\Delta b(\alpha)}{2R}T - \frac{\Delta c(\alpha)}{6R}T^2 - \frac{\Delta d(\alpha)}{12R}T^3 \tag{11}$$

where $I_K(\alpha)$ is the constant of integration that can be obtained from Eq 9 by using $T = T^{\circ}$. Finally, using eq 11 in eq 2 gives

$$\ln K(\alpha) = I_K(\alpha) - \frac{I_H(\alpha)}{RT} + \frac{\Delta a(\alpha)}{R}\ln T + \frac{\Delta b(\alpha)}{2R}T + \frac{\Delta c(\alpha)}{6R}T^2 + \frac{\Delta d(\alpha)}{12R}T^3 \tag{12}$$

EXPERIMENTAL RESULTS AND DISCUSSION

Experimental results for the thermodynamic equilibrium constant were obtained from the disassociation of ETBE (obtained from Aldrich Chemical, 99% purity) with Amberlyst 15 ion exchange resin as a catalyst, in a 6 cm. stainless steel reactor tube (diameter 1/4"). The catalyst (obtained from Sigma Chemical Co.) was prepared by first washing the resin with distilled water, followed by 0.1 M nitric acid and dried overnight

in a vacuum oven at 110 °C. After filling the stainless steel reactor tube with liquid ETBE, approximately 10 - 20 grains (particle size, 16 - 50 mesh) of Amberylst 15 were added and the tube was sealed and placed in a temperature controlled water bath. The experiments were performed over the range of temperatures, 20 - 60 °C. The reactor system was allowed to equilibrate for at least 24 hours before sampling, and for substantially longer periods for temperatures under 35° C. At least three liquid samples were taken by a syringe through a septum and analyzed by a Perkin Elmer AutoSystem Gas Chromatograph with helium as the carrier gas (25 ml/min) using a PORAPAK R column (6'x1/8") at an oven temperature of 170 °C. The GC was calibrated for ETBE over a wide range of compositions for accurate analysis, and, consequently, the maximum error in the measurement of its mole fraction was estimated to be ±0.005. Activity coefficients were calculated making use of the UNIFAC method.

Thermochemical data given in Table 1 for the liquid-phase system was obtained from the TRC Thermodynamics Tables (1986). The coefficients for the third order polynomial in temperature, eq 8, were fitted to the experimental data for ethanol and isobutylene taken from Gallant (1968). However, the liquid-phase Gibbs energy of formation for isobutylene was not found in the literature and, therefore, was calculated making use of a form of the Clausius-Claperyon equation.

Table 1. Liquid Phase Thermochemical Data* and Liquid Phase Heat Capacity Equation Coefficients

Component	Heat Capacity Coefficients of Equation 10				ΔG°_{fT},	ΔH°_{fT},
	a_j	b_j	c_j	d_j	kJ/mol	kJ/mol
Isobutylene	35.44	0.802	-3.124E-3	5.045E-6	60.672[a]	-37.7
Ethanol	29.01	0.2697	-5.658E-4	2.079E-6	-174.8[b]	-277.51
ETBE	40.418	0.7532	-1.053E-3	1.8066E-6	-126.8	-357.5[c]

* TRC Thermodynamics Tables (1986)

[a] not given in literature, calculated by Clausius-Claperyon equation

[b] from CRC Handbook (1992)

[c] adjusted value

Initially, the literature value of the standard liquid-phase enthalpy of formation of ETBE was taken from the TRC Thermodynamics Tables (1986) as -351.5 kJ/mol, but was subsequently adjusted to -357.5 kJ/mol, or by about 1.7%. Figure 1 shows the liquid-phase thermodynamic equilibrium constant as a function of temperature calculated using liquid-phase thermochemical data (Table 1), with the adjusted and non-adjusted values for the standard enthalpy of formation of ETBE. The expression resulting from the adjusted value is

$$\ln K(l) = 10.387 + \frac{4060.59}{T} - 2.89055 \ln T - 0.0191544\, T + 5.28586 \times 10^{-5} T^2 - 5.32977 \times 10^{-8}\, T^3 \qquad (13)$$

As shown in Figure 2, eq 13 agrees quite well with experimental data from not only this work, but also those reported by Vila et al. (1993) and by Françoisse and Thyrion (1991), and is, consequently, the recommended expression.

CONCLUSIONS

A thermodynamic analysis of the ETBE liquid-phase reaction is done to obtain an expression for the liquid-phase equilibrium constant (eq 13) that agrees well with experimental data. The analysis is based on the thermodynamic data reported in the literature, with the exception of ETBE, for which complete data are not yet available. Consequently, the standard enthalpy of formation of ETBE was adjusted to -357.5 kJ/mol, as compared with a reported value of -351.6 kJ/mol, in order to obtain better agreement with data over a range of temperatures. The liquid-phase equilibrium constant was also calculated using gas-phase thermochemical data, with good results as shown by Jensen and Datta (1994), further supporting the adjusted value for the standard enthalpy of formation of ETBE.

Figure 1. Thermodynamic Equilibrium Constant with Adjusted and Nonadjusted Liquid-Phase Enthalpy of Formation of ETBE

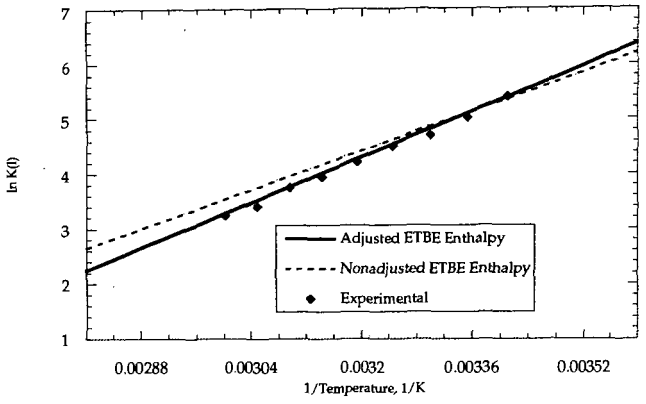

Figure 2. Experimental and Literature Data Compared with the Predicted Liquid-Phase Equilibrium Constant

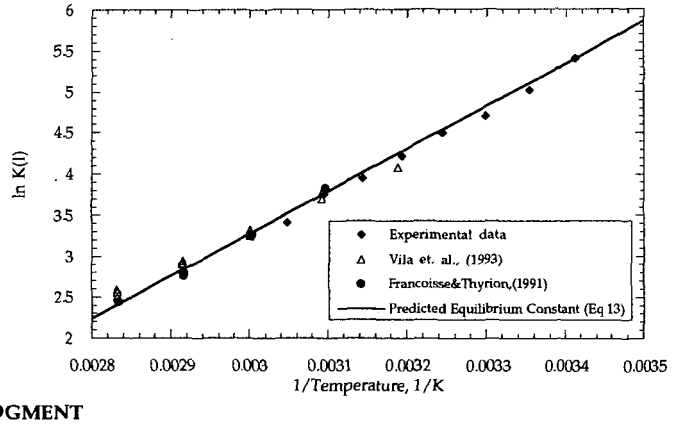

ACKNOWLEDGMENT

The funding provided for this work by the Iowa Corn Promotion Board and the National Renewable Energy Laboratories is gratefully acknowledged.

NOMENCLATURE

a_j, b_j, c_j, d_j= coefficients of molar heat capacity expression, eq 10
a_j = activity of species j, $\equiv \gamma_j x_j$
$C^{\circ}_{pj}(\alpha)$ = molar heat capacity of species j in phase α, J/mol-K
ETBE = ethyl *tert*-butyl ether
I_H = constant of integration in the Kirchoff equation, eq 11
I_K = constant of integration in v'ant Hoff equation, eq 12
$K(l)$ = liquid-phase thermodynamic equilibrium constant
$K(\alpha)$ = thermodynamic equilibrium constant for phase α
K_γ = equilibrium constant in terms of activities, eq 1
K_x = equilibrium constant in terms of mole fractions, eq 1
l = liquid phase
n = total number of species
P = pressure, bar
P° = standard pressure, 1 bar

R = gas constant, 8.3143 J/mol-K
S°_{jT} = standard entropy of species v at the temperature T, J/mol-K
T = temperature, K
T° = standard temperature, 298.15 K
$\tilde{V}_j(l)$ = liquid molar volume of species j, mL/mol
VOC = volatile organic compound
x_j = mole fraction of species j

Greek letters

α = phase (g or l)
γ_j = activity coefficient of species j
$\Delta G^{\circ}_{fjT}(\alpha)$ = standard Gibbs energy of formation of species j in phase α at temperature T, kJ/mol
$\Delta G^{\circ}_{T}(\alpha)$ = standard Gibbs energy change for reaction in phase α at temperature T, eq 3, kJ/mol
$\Delta H^{\circ}_{fjT}(\alpha)$ = standard enthalpy of formation of species j in phase α at temperature T, kJ/mol
$\Delta H^{\circ}_{T}(\alpha)$ = standard enthalpy change for reaction in phase α at temperature T, eq 5, kJ/mol
ΔS°_{T} = standard entropy change for reaction at temperature T, J/mol-K
ν_j = stoichiometric coefficient of species j in reaction

Subscripts

e = at equilibrium
f = of formation
j = of species j
T = at temperature T
T° = at standard temperature

Superscripts

$^{\circ}$ = at standard state (1 bar; also ideal gas for gas phase)

LITERATURE CITED

CRC Handbook of Chemistry and Physics, Lide, D. Ed., CRC: Boca Raton, 73rd Edition, 1992.

Françoisse, O.; Thyrion, F. C. Kinetics and Mechanism of Ethyl tert-Butyl Ether Liquid-phase Synthesis. *Chem. Eng. Process.* **1991**, *30*, 141-149.

Gallant, R. *Physical Properties of Hydrocarbons*, Gulf Publishing: Houston, Volume 1, 1968.

Iborra, M.; Izquierdo, J.; Tejero, J. F.; Cunill F. Equilibrium Constant for Ethyl tert-Butyl Ether Vapor-Phase Synthesis. *J. Chem. Eng. Data.* **1989**, *34*, 1-5.

Jensen, K.; Datta, R. Equilibrium Thermodynamic Analysis of the Liquid-Phase Ethyl *tert*-Butyl Ether (ETBE) Reaction. *Ind. Eng. Chem. Res.* Submitted **1994**.

Lucht, G. Ethanol Approval Creates Hugh Sighing Sound, *Iowa Farmer Today*_ Dec. 25, 1993, (10), 1-2.

Oxy-Fuel News. ARCO Chemical, Coastal to Produce ETBE in Texas. Vol IV, No. 22, Sept. 7, **1992**,1.

Reid, R.; Prausnitz, J.; Poling, B. *The Properties of Gases & Liquids*, McGraw-Hill: New York, Fourth Edition, 1987.

Reisch, M. Top 50 Chemicals Production Rose Modestly Last Year, *C&EN* **1994**, April 11, 12-15.

TRC Thermodynamics Tables, Hydrocarbons and Nonhydrocarbons, Thermodynamics Research Center, Texas A&M University, 1986.

Vila, M.; Cunill, F.; Izquierdo, J. F.; Tejero, J.; Iborra, M. Equilibrium Constants For Ethyl *tert*-Butyl Ether Liquid-Phase Synthesis. *Chem. Eng. Comm.* **1993**, *124*, 223-232.

METHANOL SYNTHESIS IN A TRICKLE BED REACTOR

by Jianhua Wang, Sinoto Tjandra, Rayford G. Anthony, and Aydin Akgerman
Department of Chemical Engineering
Texas A&M University
College Station, TX 77843-3122

Keywords: Methanol synthesis, trickle bed reactors, syngas

INTRODUCTION

The conversion of synthesis gas to methanol is practiced commercially in gas phase fixed bed reactors over a $Cu/Zn/Al_2O_3$ catalyst. However, because of the highly exothermic nature of the synthesis reactions, heat dissipation has been a bottleneck in the reactor design and process configuration. Moreover, coal-derived synthesis gas, having a low H_2/CO ratio, is not suitable for use in fixed bed reactors because of coke deposition. Trickle bed reactors combine advantages of both gas phase fixed bed and slurry reactors. With a liquid phase trickling over catalyst particles, the heat removal in trickle bed reactors is much more efficient compared to fixed bed reactors, which makes trickle bed reactors suitable for direct use of the coal-derived synthesis gas. On the other hand, like fixed bed reactors, trickle bed reactor can operate at high gas space velocities and have high conversions per pass.

EXPERIMENTAL

Figure 1 shows a schematic diagram of trickle bed reactor system. Feed gas to the reactor consists of pure H_2 and a mixture of CO and CO_2 with a constant CO/CO_2 ratio of 0.9 throughout the study. The feed gas streams flow through a guard bed paced with activated carbon and molecular sieve having a particle size of 0.16 cm to remove any carbonyl that would poison the catalyst. Gas flow rates are controlled with Brooks model 5850E mass flow meters. To enhance mixing, the gas streams pass through a bed of glass beads prior to the reactor. A mineral oil consisting of saturated aliphatic and naphthenic hydrocarbons supplied by Witco Co. is introduced with a Milton Roy model DE-1-60P pump at the reactor inlet, along with the gas mixture. The oil flow rate is maintained at 2.5 kg/(m^2 s) to ensure sufficicnt catalyst wetting.

The reactor is a 316 stainless steel tube with an ID of 0.96 cm, an OD of 1.20 cm, and length of 25 cm. It is mounted vertically in a bed of aluminum pellets. The reactor bed is divided into three sections. Prior to and after the 5.6 cm catalyst bed are 6.0 and 13.4 cm supporting sections filled with 0.2 cm diameter glass beads. The reactor is heated by a heating block and temperature in the reactor is controlled by Omega model 6100 temperature controller. Temperature in the catalyst bed is measured with a thermocouple inserted in the bed, while the pressure in the reactor is maintained at 5.2 MPa with a Grove model 91W back pressure regulator. A relief valve set to 10.6 MPa is placed before the reactor to prevent uncontrolled pressure rise in the system. The reactor is packed with 7 grams of crushed $CuO/ZnO/Al_2O_3$ alcohol synthesis catalyst (United Catalyst L-951) having particle size of 500-600 μm. In situ reduction is carried out according to the procedure described by Sawant et al. (1987).

Reactor effluent passes through the back pressure regulator where the pressure is reduced to atmospheric pressure prior to the gas-oil separator. The separator is heated to 100-110 °C with a heating tape, and the temperature is controlled with a Omega model 6100 temperature controller. The oil collected at the bottom of the separator is recycled back to the reactor. After the gas-oil separator, a Gow Mac 550 gas chromatograph equipped with a HP 3969 integrator is installed to check the steady state of the reaction. Methanol, water, and other products are separated from the unreacted gas by using a series of condensers immersed in a dry ice/acetone bath. The condensate is analyzed off-line on the Gow Mac 550 gas chromatograph. The tail gas then passes through a soap bubble meter to record the volumetric flow rate before vented to the hood. A sample of the tail gas is taken at the sample port after the condensers and injected into a Carle gas chromatograph, equipped with a Varian 4290 integrator, to analyze its composition.

REACTOR MODELS

To develop reactor models, the following assumptions have been made: (i) the gas phase is in plug flow and the liquid phase is in axially dispersed flow, (ii) the gas superficial velocity varies throughout the reactor, but the liquid superficial velocity is constant, (iii) catalyst particles have spherical geometry, (iv) the surface of each particle is partially wetted, but the pores inside the

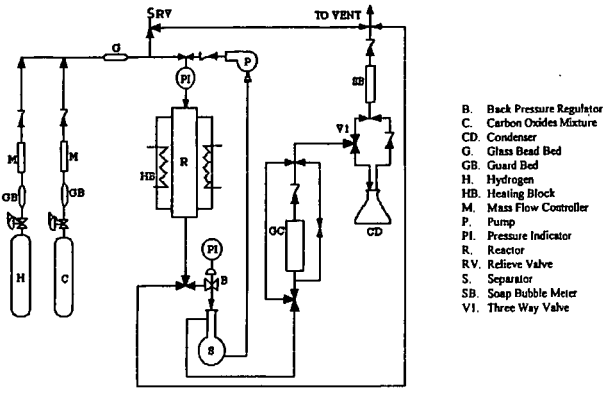

Figure 1. Experimental apparatus.

particle are fully filled with the liquid, (v) at any point inside the reactor, temperatures in the gas, liquid, and solid phases are equal, (vi) methanol synthesis occurs only through the CO hydrogenation to methanol, and the water gas shift reaction is in dynamic equilibrium. With the above assumptions, a three phase reactor model was developed which incorporated plug flow, axial dispersion, mass transfer resistances between the gas and liquid phases, interparticle and intraparticle diffusion resistances, heat transfer, and pressure drop as well as two surface reactions. This reactor model equations with proper boundary conditions consist of a group of coupled, nonlinear partial differential and algebraic equations, and it is mathematically a two-point boundary-value problem.

Another two, simplified two-phase reactor models for trickle bed reactors are also developed for the purpose of comparison. In the first two phase, simplified reactor model, the two-phase model I, the assumption of no interparticle and intraparticle diffusion resistances are added to the three phase reactor model. Mathematically, the reactor model consists of a group of coupled, nonlinear ordinary differential and algebraic equations, and it is also a two-point boundary-value problem. In the second two phase, simplified reactor model, the two-phase model II, it is further assumed that: there is no mass transfer resistance between the gas phase and the liquid phase; both the gas and liquid phase are in plug flow; only the CO hydrogenation to methanol reaction occurs in the synthesis process; the reactor operates isothermally and there is no pressure drop. The model equation is mathematically a initial value problem.

For the system operated under typical commercial conditions, it was shown that assuming a perfect mixture gave better results than the Redlich-Kwong equation of state and similar results compared with the virial equation truncated after the second virial coefficient. In this study, the assumption of a perfect gas mixture is made. Parameters associated with model equations are mass and heat transfer coefficients, effective diffusion coefficient, Henry's constants, wetting coefficient, liquid axial dispersion coefficient and hold-up, as well as those parameters in kinetic rate expressions. An empirical kinetic rate expressions developed by Al-Adwani (1992) was used in the simulation. The expression was fitted from experimental data obtained in slurry reactors over a commercial $CuO/ZnO/Al_2O_3$ catalyst. All other model parameters were estimated independently from either published correlations or literature data.

The model equations in two-point boundary-value problem were first rearranged into a dimensionless form, and transformed into linearized algebraic equations with combination of orthogonal collocation and quasi-linearization, and solved with an iteration scheme. In this study, 8 and 6 interior collocation nodes were used for longitudinal direction of the reactor and radial

direction of catalyst particles, respectively. The initial value problem was solved with Gear's BDF method.

RESULTS AND DISCUSSION

It was shown that the reactor operated in the trickle flow regime according to the published criterion for maintaining trickle flow regime. The time on stream study showed that catalyst activity decreased sharply during the first 150 hours, after which it had reached a steady state for 510 hours during a total 660 hours operation. Experiments were performed at three temperatures, 235, 250, and 260 °C; and a gas space velocity range of 5,200 to 35,000 h^{-1} at 250 °C and 5,200 to 14,000 at 235 and 260 °C. Gas space velocity is defined as volumetric flow rate divided by volume of catalyst calculated at the standard conditions through this study.

Figure 2 shows a comparison between predicted and experimental CH_3OH productivity under different gas space velocity. CH_3OH productivity is defined as methanol production rate in moles per hour divided by total weight of catalyst loaded. In this plot, the reaction temperature, T_w, is 250 °C, and the hydrogen to carbon oxides ratio, $H_2/(0.9CO+0.1CO_2)$, is 1. The solid circles represent experimental CH_3OH productivity (Legend heading EXP). The short dash line denotes predicted CH_3OH productivity from the two-phase model II (Legend heading M2PHS(II)), in which mass transfer resistance between the gas and liquid phases as well as interparticle and intraparticle diffusion resistances are neglected. The long dash line designates the prediction of CH_3OH productivity from the two-phase model I (Legend heading M2PHS(I)), in which interparticle and intraparticle diffusion resistances are not accounted for. The solid line marks the predicted CH_3OH productivity from the three-phase reactor model (Legend heading M3PHS), which considers both mass transfer resistance between the gas and the liquid phases and interparticle and intraparticle diffusion resistances.

Figure 2 shows that the difference between the predicted CH_3OH productivity from the three-phase reactor model and from the two-phase models is greater than the difference between the predicted results obtained from the two two-phase reactor models. As expected, the two-phase model II always gives the highest CH_3OH productivity since this reactor model considers no mass transfer resistance among the gas, liquid, and solid phases, and, on the other hand, the three-phase reactor model predicts the lowest CH_3OH productivity because this reactor model considers not only mass transfer resistance between the gas and liquid phases but also interparticle and intraparticle mass transfer resistances. Accordingly, the two-phase model I that accounts for only mass transfer resistance between the gas and liquid phases gives intermediate CH_3OH productivity between the values obtained from the other two reactor models.

Figures 3 and 4 exhibit comparison between predicted and experimental CO and H_2 conversions under different gas space velocities at the same operating conditions as in Figure 2. Likewise, the highest predicted CO and H_2 conversions come from the two-phase reactor model II, and the lowest conversions from the three-phase reactor model. However, much lower values of H_2 conversion than the experimental values predicted from all three reactor models at gas space velocities greater than 20,000 h^{-1} result from uncertainty of the measurement of H_2 conversion. Figures 3 and 4 also show that there are obvious differences between predicted CO and H_2 conversions from the three-phase reactor model and ones from the two-phase reactor models. It should also be noted that in the simulation, all model parameters as well as the kinetic rate equations were estimated independently without using any experimental data obtained in the reactor studied, and that there was an average error of 11% associated with the evaluation of kinetic parameters for the kinetic rate expression. Moreover, with increasing catalyst sizes, especially when commercial size catalyst are packed, it is anticipated that both mass transfer resistance between the gas and liquid phases and interparticle and intraparticle diffusion resistances plays an more important role. Hence, it is necessary to utilize the three-phase reactor model to predict the performance of trickle bed reactor packed with commercial size catalysts.

Figures 5 and 6 compare the predicted results from the three-phase reactor model with the experimental values at the same temperature of 250 °C but two different $H_2/(0.9CO+0.1CO_2)$ ratios of 0.5 and 2.0, respectively. In these figures, the scatter points marked by triangles and diamonds (Legend heading EXP) symbolize the experimental measurements. The line signifies the model predictions from the three-phase non-isothermal reactor model (Legend heading M3PHS). The ratios in the parenthesis following the legend headings of EXP and M3PHS designate $H_2/(0.9CO+0.1CO_2)$ ratios employed in the experiments and modeling. Figure 5 shows

that the three-phase reactor model under-predicts CH_3OH productivity except at gas space velocities lower than 8,000 h^{-1}. However, Figure 6 shows that the predicts CO conversion matches experimental values well at the $H_2/(0.9CO+0.1CO_2)$ ratios of 0.5 and 2.0 under a broad range of gas space velocities. It should be noted that the stoichiometric ratio of H_2 to CO in the CO hydrogenation reaction is 2.0. Hence, at the $H_2/(0.9CO+0.1CO_2)$ ratio of 2.0 that is close to the stoichiometric ratio, CO conversion can go as high as 46% at low gas space velocities; then, the conversion declines quickly with increasing gas space velocities. On the other hand, at $H_2/(0.9CO+0.1CO_2)$ ratios less than 2.0, H_2 is a limiting reactant and CO is in excess; therefore, CO conversion is substantially lower than one obtained at the $H_2/(0.9CO+0.1CO_2)$ ratio of 1 under low gas space velocities.

CONCLUSIONS

Even though the two-phase reactor models are capable of predicting the experimental results obtained in a laboratory trickle bed reactor, the three-phase reactor model is recommended for predicting the performance of trickle bed reactors packed with commercial size catalysts, with which severe diffusion effect could be conceived.

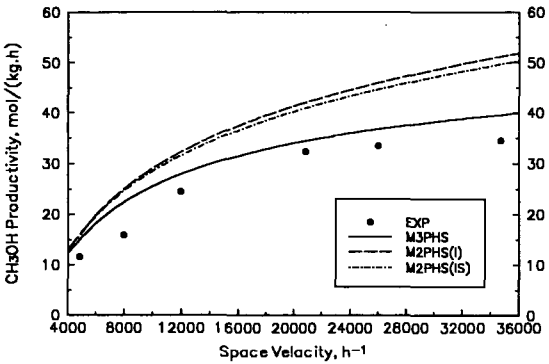

Figure 2 Comparison between predicted and experimental CH_3OH productivity at T_w=250 °C and $H_2/(0.9CO+0.1CO_2)$=1.

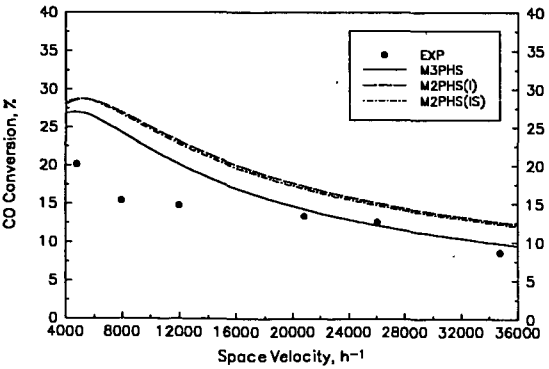

Figure 3 Comparison between predicted and experimental CO conversion at T_w=250 °C and $H_2/(0.9CO+0.1CO_2)$=1.

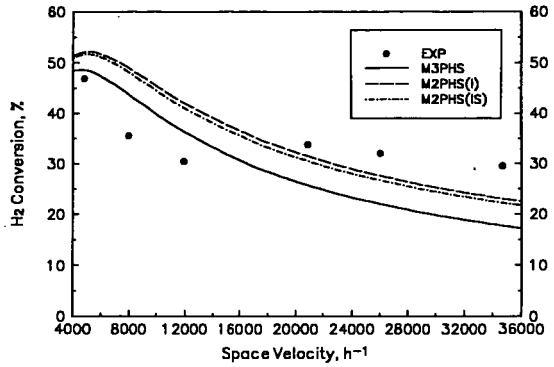

Figure 4 Comparison between predicted and experimental H_2 conversion at T_w=250 ℃ and $H_2/(0.9CO+0.1CO_2)=1$.

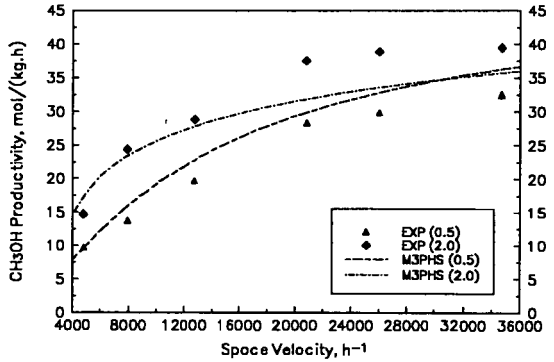

Figure 5 Comparison between predicted and experimental CH_3OH productivity at T_w=250 ℃ and $H_2/(0.9CO+0.1CO_2)=0.5$ and 2.0, respectively.

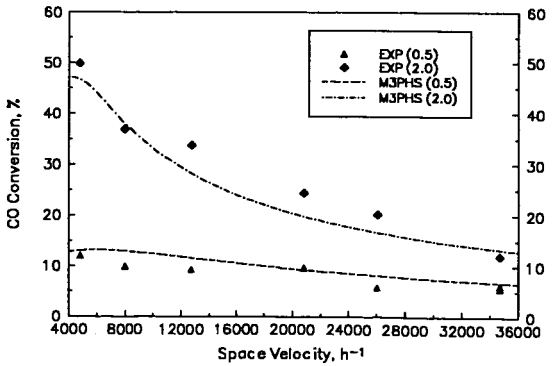

Figure 6 Comparison between predicted and experimental CO conversion at T_w=250 ℃ and $H_2/(0.9CO+0.1CO_2)=0.5$ and 2.0, respectively.

A MODEL FOR LIQUID PHASE METHANOL SYNTHESIS PROCESS IN A COCURRENT FLOW ENTRAINED REACTOR

P. Vijayaraghavan, Conrad J. Kulik*, and Sunggyu Lee+

Process Research Center
Department of Chemical Engineering
The University of Akron
Akron, OH 44325-3906

*Fuel Science Program
Electric Power Research Institute
3412 Hillview Avenue
Palo Alto, CA 94304

ABSTRACT

Experimental studies on the liquid phase synthesis of methanol were performed in an entrained reactor. In this three-phase process, syngas reacts in the presence of the catalyst-oil slurry, to form the product methanol. The effect of various operating conditions which included reactor temperature, pressure, flow rates of slurry and syngas, slurry holdup tank pressure, syngas composition and catalyst loadings, on the reactor productivity were studied. An overall experimental reaction rate model to predict the productivity of methanol using the operating conditions as the variables was developed, and the results were compared with the experimental data.

A computer model was also developed that predicts the reactivity of all species involved in the methanol synthesis process in an entrained reactor, from inlet conditions. This model incorporates the kinetic rate expression and the gas-liquid mass transfer correlation that was developed for the methanol synthesis process in a liquid entrained reactor. The rate of production of methanol predicted by this computer model agreed well with the experimental results. The overall experimental reaction rate model and the computer model assists in the development, scale-up and commercialization of the liquid phase methanol synthesis process in an entrained reactor.

+ To whom all correspondence should be directed.

Keywords: Liquid phase methanol synthesis process, Entrained slurry reactor, Reactor modeling

SIGNIFICANCE OF THE LIQUID PHASE METHANOL SYNTHESIS PROCESS

The liquid-phase methanol synthesis (LPMeOH) process that was developed by Chem Systems, Inc. in 1975 (Sherwin and Blum, 1979), was a three phase process that provided improved reactor stability and the compatibility of using a synthesis gas mixture with a higher CO content than H_2. However this process is not limited to CO-rich syngas only. The advantages of such a process in terms of reactant gas compositions include the use of coal derived feedstocks, and as a result, the process can be additionally significant in the production of clean liquid fuels (Lee, 1990).

The commercial reactor proposed for the LPMeOH process is an entrained reactor. In an entrained reactor, the catalyst particles in powder form are uniformly suspended in the liquid (oil) and this catalyst-oil slurry is continuously recirculated by a pump through a tubular reactor. Contact with the syngas is made by feeding the gas cocurrently with the upward flow of slurry (Vijayaraghavan and Lee, 1992). The inert liquid provides a much larger thermal mass than the vapor medium, thus facilitating the easier control of temperature by absorbing the exothermic heat generated during the methanol reaction.

The objective of this study is to develop an overall experimental reaction rate model to predict the production of methanol from operating conditions, and to develop a computer model to predict the reactivity of all species involved in the methanol synthesis process in a liquid entrained reactor, from inlet conditions. Such information is essential for the design, development and scale-up of the methanol synthesis process in a liquid entrained reactor.

MINI-PILOT PLANT ENTRAINED SLURRY REACTOR SYSTEM

A laboratory scale, continuous, mini-pilot plant was designed and built to carry out methanol synthesis research in a liquid entrained reactor (Vijayaraghavan, 1994). The details of the entrained reactor system and its peripherals is shown in Figure 1. The entrained reactor is a 76.2 cm. long stainless steel tube. Its outer diameter is 1.31 cm. The

feed gas and the catalyst-oil slurry are introduced cocurrently from the bottom of the reactor. This provides effective dispersion of gas bubbles and along with the high flow rate of slurry, ensures a good suspension of solid particles in liquid. The reactor is equipped with an external heating device, capable of raising the temperature of the fluids in the reactor to the desired operating temperature.

Syngas is passed to the reactor at a desired flow rate by a mass flow controller. A pneumatically operated air-to-close back pressure control valve with positioner, connected to a pressure controller, maintains the entrained reactor at the desired pressure. The slurry is recirculated in the entrained reactor by a specially designed plunger type reciprocating slurry pump, which is capable of handling slurries containing as high as 40 wt.% of metallic catalyst solids. The entrained reactor system is provided with a slurry holdup vessel that is thoroughly agitated by a Magnedrive impeller, to prevent the catalyst settling and agglomeration. The unreacted gases and the product vapors from the slurry holdup vessel flow to the condenser. A sample bottle is installed at the exit of the condenser. The oil free gas flows to the lower chamber of a back pressure regulator, which maintains the slurry holdup tank pressure at a lower pressure than the entrained reactor, to facilitate product flashing and thereby separating the product vapors from the catalyst-slurry system. The flow rate of the vent gas is measured using a wet test meter. The on-line analyses of the feed and product gases and liquid product are carried out using a gas chromatograph coupled to an integrator.

EXPERIMENTAL DESIGN AND PROCEDURE

The syngas blending and compression procedure and the catalyst activation procedure developed for low (< 25 wt. %) and high (> 25 wt. %) concentration of catalyst in slurry are published elsewhere (Sawant *et al.*, 1987; Vijayaraghavan, 1994). A FORTRAN program that was developed to compute the material balance of experiments across the reactor system is given elsewhere (Lee, 1990; Parameswaran, 1987).

In order to develop an overall reaction rate model and a computer model to predict the reactivity of all species involved in the methanol synthesis process in a liquid entrained reactor, a statistical design of experiments was established and performed. From initial studies, it was found that the reactor temperature, pressure, syngas and slurry flow rates, and slurry hold-up tank pressure, are the important variables. A fractional factorial (2^{5-2}) design was used and is explained elsewhere (Vijayaraghavan, 1994). The high and low levels for each variable were chosen so that commercially interesting conditions would lie in the middle of the design. The levels of the variables are shown in Table I. These experiments were repeated for three different catalyst loadings by weight (10 %, 25 %, and 35 %) in slurry, to cover the kinetic and mass transfer controlling regimes.

ANALYSIS OF EXPERIMENTAL DATA

Experiments were performed according to the design mentioned earlier and the data obtained for 10%, 25% and 35% concentration by weight of catalyst in slurry were analyzed to develop an overall reaction rate expression model and a computer model that would predict the production of methanol in an entrained reactor, for any given operating condition. The data points cover 2 levels of reactor temperature, reactor pressure, syngas flow rate, slurry holdup tank pressure, slurry flow rate, syngas composition, and 3 levels of catalyst concentration by weight in slurry.

Overall Rate Expression for LPMeOH Process in an Entrained Reactor

The development of an overall rate model is essential to predict the production of methanol in an entrained reactor, for any given operating condition. The 6 variables used for analyzing the data included reactor temperature, pressure, syngas flow rate, slurry holdup tank pressure, slurry flow rate, and catalyst concentration by weight in slurry. The overall rate expression for methanol productivity was developed using data described in detail elsewhere (Vijayaraghavan, 1994). The 6 variables were correlated using a SAS Program (PROC GLM) featuring a regression-correlation method that uses the principle of least squares to fit general linear models and generates the estimates of the unknowns.

The overall reaction rate expression for methanol productivity in an entrained reactor for the available data, can be best represented by the following statistical correlation model:

$$R_{MeOH} = 0.0027 \times T - 0.039 \times P - 24.75 \times F_g + 249.30 \times C + 7.6 \times 10^{-5} \times T \times P + 0.044 \times T \times F_g - 0.445 \times T \times C + 0.0026 \times P \times F_g + 9.7 \times 10^{-6} \times P \times P_H - 0.03 \times P \times C - 0.003 \times F_g \times P_H + 0.025 \times F_g \times F_s + 0.405 \times F_g \times C + 5.7 \times 10^{-4} \times P_H \times C \quad \ldots (1)$$

where R_{MeOH}, T, P, F_g, P_H, F_s, and C represent the rate of methanol production (mol/kg.cat-h), reactor temperature (K), reactor pressure (psi), syngas flow rate (SLPM),

slurry holdup tank pressure (psi), flow rate of slurry (l/h), and catalyst concentration in slurry (weight fraction), respectively.

It is seen from Figure 2 that the rate of methanol production predicted by Equation (1), match very well with the experimental rate data. It is observed that the average error between the experimental and the predicted rate values is 9.5%. Considering the range of practical experimental operating conditions and the inherent experimental error, the average deviation of the model seems quite good.

The overall rate expression shown in Equation (1) can help to predict the methanol production for any given operating condition, and would be extremely useful for process design, development and scale-up computations.

Computer Modeling of the Liquid Entrained Reactor

Modeling of the liquid entrained reactor was carried out to predict the reactor productivity from inlet conditions. This computer program can accurately predict the multicomponent phase equilibria, ultimate chemical equilibria, and compositions of all reactant and product species exiting in the entrained reactor. Intrinsic reaction rate expressions and overall rate expressions based on the gas-liquid mass transfer correlation were developed earlier (Vijayaraghavan, 1994).

For CO-rich syngas, the intrinsic reaction rate expression is:

$$R_{MeOH} = 0.75 \times 10^{10} \, Exp(-20500/RT) \, (C_{H2} - C_{H2}^{eq}) \qquad \ldots (2)$$

For H_2-rich syngas, the intrinsic reaction rate expression is:

$$R_{MeOH} = 0.41 \times 10^{10} \, Exp(-20500/RT) \, (C_{H2} - C_{H2}^{eq}) \qquad \ldots (3)$$

The overall reaction rate expression in terms of gas-liquid mass transfer coefficient is (Lee, 1990):

$$R_{MeOH} = (V_{oil}/W) \, (M^{-1}) \, (C_{H2} - C_{H2}^{eq}) \qquad \ldots (4)$$

$$M = (V_{oil}/W) \, (1/k_r) + (1/K_{Li}a_B) \qquad \ldots (5)$$

In Equations (2), (3), (4), and (5), R, V_{oil}, W, $K_{Li}a_B$, k_r, C_{H2}, and C_{H2}^{eq} represent the universal gas constant (l-atm./mol-K), volume of oil at operating conditions (l), mass of catalyst in slurry (kg), overall gas-liquid mass transfer coefficient (1/h), intrinsic reaction rate constant represented by Equations (2) and (3), and the physical and chemical equilibrium concentrations of hydrogen in oil (mol/l), respectively.

The overall gas-liquid mass transfer coefficient was best represented by the following correlation:

$$N_{Sh} = 1.07 \times 10^{-9} \, . \, N_{Sc}^{0.5} \, . \, N_{Bo}^{1.12} \, . \, N_{Ga}^{1.13} \, . \, N_{Fr}^{0.08} \, . \, (U_l/U_g)^{0.44} \, . \, \varepsilon_g^{1.1} \qquad \ldots (6)$$

where N_{Sh}, N_{Sc}, N_{Bo}, N_{Ga}, and N_{Fr} represent the Sherwood Number ($K_{Li}a_B \, d_c^2 \, / \, D_{H2,l}$), Schmidt Number ($\mu_l \, / \, (\rho_l \, D_{H2,l})$), Bond Number ($d_c^2 \, \rho_l \, g \, / \, \sigma$), Galileo Number ($d_c^3 \, \rho_l^2 \, g \, / \, \mu_l^2$) and the Froude Number ($U_g \, / \, (g \, d_c)^{0.5}$), respectively. The gas phase holdup is best represented by the following expression (Vijayaraghavan, 1994):

$$\varepsilon_g = 0.672 \, . \, (U_g . \mu_l/\sigma)^{0.58} \, . \, (\mu_l^4 \, g/(\rho_l \, \sigma^3)^{-0.13} \, . \, (\rho_g \, /\rho_l)^{0.06} \, . \, (\mu_g \, / \, \mu_l)^{0.11} \qquad \ldots (7)$$

In Equations (6) and (7) d_c, $D_{H2,l}$, μ_l, μ_g, ρ_l, ρ_g, σ, U_l, U_g, ε_g and g represent the column diameter, diffusivity of hydrogen in liquid, viscosity of slurry, viscosity of gas, density of slurry, density of gas, surface tension of oil, velocity of slurry, velocity of gas, gas holdup and gravitational acceleration, respectively.

The development of Equations (2) - (7) used in the computer modeling of the entrained reactor for the liquid phase methanol synthesis process, are described elsewhere (Vijayaraghavan, 1994). The length of the entrained reactor is divided into a number of segments and the concentration of each species in the liquid and vapor phase in each segment is calculated after the physical and chemical equilibrium criteria are met, using computer programs developed earlier (Ko *et al.*, 1987; Lee, 1990). Gas phase holdup, vapor phase compositions, pressure, temperature, volume of oil, and mass of catalyst in each segment of the reactor are required as input data for the next segment in this program. The ratios of reaction of hydrogen, carbon monoxide, carbon dioxide and water with respect to methanol were averaged for the entire data for facilitating modeling purposes. The number of moles of each species entering the (i+1)-th segment of the reactor, is the difference between the number of moles of that species entering the i-th segment and the number of moles of that species reacting in the i-th segment. Thus the number of moles of each reactant and product species entering and exiting each reactor segment is computed cumulatively, and hence the final exiting moles of each species in the reactor is determined.

The data used for the entrained reactor modeling purposes are described elsewhere (Vijayaraghavan, 1994). It is seen from Figure 3 that the experimental data and the modeling results agree well with each other, and the average error between the results is less than 14%. Since hydrogen is no longer the limiting reactant for H_2-rich syngas operating condition, the concentration difference term ($C_{H2} - C^{eq}_{H2}$) plays an important role in the significant deviations observed in Figure 2 for certain experimental runs (5, 11, 16). The average deviation of the computer model seems good considering the extensive thermodynamic computations incorporated in the model, the experimental error, and the wide range of operating conditions employed.

This modeling of the entrained reactor can help to predict the production of methanol for any given inlet conditions and would be extremely useful for the optimization, improvement and scale-up of the methanol synthesis process in a liquid entrained reactor.

CONCLUSION

An overall reaction rate model that could predict the productivity of methanol for any given operating conditions, was successfully developed for the liquid phase methanol synthesis process in an entrained reactor. A computer model that would predict the reactivity of all chemical species involved in the methanol synthesis process in an entrained reactor, from inlet feed conditions was successfully developed. Data covering a wide range of operating conditions, including varying composition of syngas and catalyst loadings, has been used to develop the overall reaction rate model and the computer prediction model. The results obtained could be of great significance in the design, development, scale-up and commercialization of the methanol synthesis process in a liquid entrained reactor.

REFERENCES

Ko, M. K., Lee, S., and Kulik, C. J., 1987. "Multicomponent Physical Equilibrium of Liquid Phase Methanol Synthesis", Energy and Fuels, 1(2), 211-216.

Lee, S., 1990. Methanol Synthesis Technology, CRC Press, Boca Raton, FL.

Parameswaran, V. R., 1987. "Roles of Carbon Dioxide and Water in the Liquid Phase Methanol Synthesis Process", Ph. D. Dissertation, The University of Akron.

Sawant, A. V., Ko, M. K., Parameswaran, V. R., Lee, S., and Kulik, C. J., 1987. "In-Situ Reduction of a Methanol Synthesis Catalyst in a Three Phase Slurry Reactor", Fuel Sci. & Tech. Int'l, 5(1), 77-88.

Sherwin, M. and Blum, D., 1979. "Liquid Phase Methanol", Final Report EPRI, AF-1292 (Project 317-2), Electric Power Research Institute, Palo Alto, CA.

Vijayaraghavan, P., and Lee, S., 1992. "Design and Operation of a Liquid Entrained Reactor Mini-Pilot Plant for Methanol Synthesis", Proceedings of the Clean Air/Clean Fuels Symposium, AIChE, New Orleans, LA.

Vijayaraghavan, P., and Lee, S., 1993. "Mini-Pilot Plant Design, and Operation of an Entrained Reactor for Liquid Phase Methanol Synthesis Process, "Fuel Sci. & Tech. Int'l, 11(2), 243-268.

Vijayaraghavan, P., 1994. "Entrained Reactor Studies on the Liquid Phase Methanol Synthesis Process", Ph.D. Dissertation, The University of Akron.

Table I

Levels of the Design Variables

Number of the Design Variable	Design Variables	(-)	(+)
1	Temperature (°C)	235	250
2	Pressure (psi)	800	950
3	Syngas Flow Rate (SLPM)	1.0	2.5
4	Slurry Holdup Tank Pressure (psi)	300	500
5	Slurry Flow Rate (l/h)	15	30

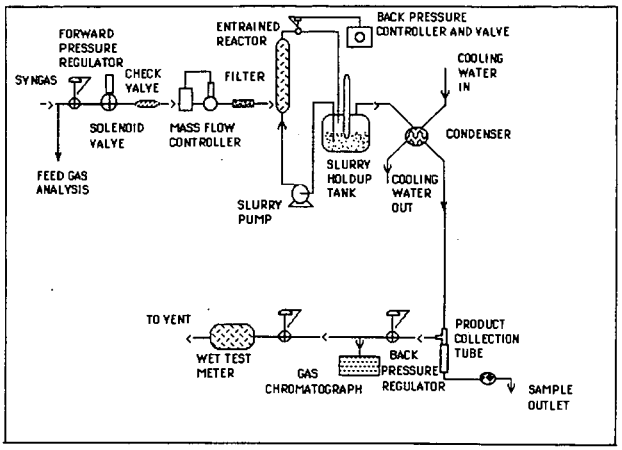

Figure 1. Liquid Entrained Reactor System and its Peripherals

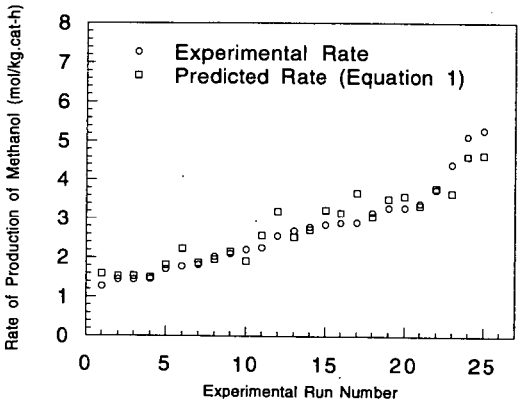

Figure 2. Comparison between Experimental Rate vs. Overall Reaction Rate Model Prediction (Equation 1)

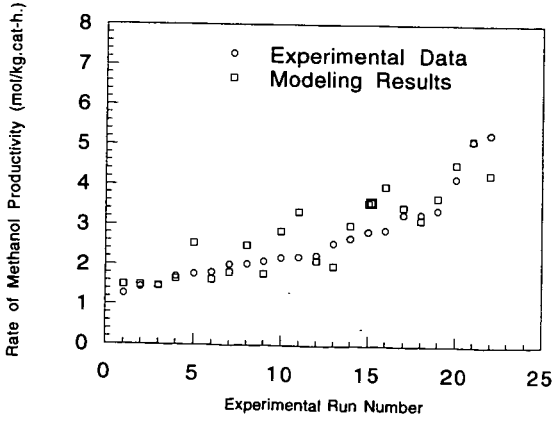

Figure 3. Comparison between Experimental Data vs. Computer Modeling Results

EVALUATION OF LOW-TEMPERATURE METHANOL SYNTHESIS IN THE LIQUID PHASE

Sei-ichi Ohyama
Atmospheric Science Department
Central Research Institute of Electric Power Industry
11-1, Iwato-kita 2 chome, Komae-shi, Tokyo 201, Japan

Keywords: Methanol synthesis, low temperature, space time yield

INTRODUCTION

Methanol has recently attracted much public attention as one of the possible alternate fuels for oil. The electric power industry is considering the introduction of methanol as a fuel for gas turbines and fuel cells. Also, coproduction of methanol and electricity in an integrated gasification combined-cycle power plant (IGCC) has been proposed for operating IGCC at levels corresponding to peak demand[1]. The electric power industry in Japan projects methanol power generation to be 1,000 MW in 2010. To employ methanol as a power plant fuel, a more efficient and more economical methanol production process, which can reduce methanol cost, is required.

Conventionally, methanol is produced in the gas-solid phase process over copper-zinc-based oxide catalysts according to the following reaction, which is highly exothermic:

$$CO + 2\,H_2 \rightarrow CH_3OH\ (g) \qquad \Delta H^\circ_{298} = -90.97\ kJ/mol \qquad (1)$$

This reaction is thermodynamically favorable at lower temperatures. Thus, if a catalyst that is highly active at low temperature is available and the reaction heat is removed efficiently, methanol production with high conversion per pass is achieved, which would result in a reduction of methanol cost.

Recently, low-temperature methanol synthesis in the liquid phase has been proposed and received considerable attention, since it has the potential to overcome problems in the conventional methanol processes. Two processes have been proposed: the Brookhaven National Laboratory (BNL) low-temperature methanol process[2,3] and the process[4-6] through methyl formate (MF) formation (hereafter referred to as "methanol synthesis *via* MF"). Methanol synthesis *via* MF is supposed to proceed by the following two reactions occurring concurrently:

$$CH_3OH + CO \rightarrow HCOOCH_3 \qquad (2)$$

$$HCOOCH_3 + 2H_2 \rightarrow 2\,CH_3OH \qquad (3)$$

The BNL process employs a homogeneous Ni catalyst and alkoxide in an organic solvent, while methanol synthesis *via* MF employs a mixture of copper-based oxide and alkoxide as a catalyst. Both processes are operated at around 373 K, where high equilibrium conversion of carbon monoxide to methanol is expected. The processes have been reported to show excellent activity even at such low temperatures.

Believing that these low-temperature methanol processes show future promise, the author has examined their catalytic activities and their possibilities as industrial processes were estimated in terms of the space time yield (STY).

EXPERIMENTAL

Experimental System

All experiments were carried out in batch operation in a 465 cm^3 stainless steel autoclave. A mixture of carbon monoxide and hydrogen with a stoichiometric ratio for methanol synthesis ($H_2/CO = 2$) was employed as feed gas. The feed gas was admitted to the reactor and pressurized to a certain pressure at ambient temperature. The reaction conditions were temperatures from ambient temperature to 433 K and initial pressures from 1.1 MPa to 5.0 MPa. The time courses of the pressure and the temperature were monitored during the run. After the run, the components of the gas phase and the liquid phase were withdrawn and analyzed by gas chromatography.

The carbon monoxide conversion and the selectivity to methanol were determined on the basis of the amount of carbon-containing products. The approximate STY was determined from the amount of methanol produced, the reaction time at which the catalyst showed a pressure decrease, and the total volume of the catalyst system. (In this paper, "catalyst system" indicates a mixture of the catalyst and the solvent.)

Catalyst Preparation

The BNL Catalysts. The BNL low-temperature methanol synthesis catalysts were prepared according to their patent reports[3]. They were prepared from three compounds, *i.e.*, sodium hydride, alcohol and metal acetate. In this work, 60 mmol of sodium hydride, 52 mmol of *tert*-amyl alcohol as the alcohol component and 2.5-30 mmol of nickel acetate (typically 10 mmol) that was fully dried and dehydrated, were employed as standard starting materials. The catalysts were suspended in a 50 or 100 cm^3 solvent (triethylene glycol dimethyl ether, *i.e.*, triglyme). A mixture of nickel acetate (10 mmol) and sodium hydride (60 mmol) was also used as a catalyst to study the active species of the catalyst.

Catalysts for Methanol Synthesis via MF. A mixture of oxide and alkoxide was employed as a catalyst for methanol synthesis *via* MF. The catalyst was suspended in triglyme (90 cm^3). Oxides used in this study (normally 4 g) were CuO (Wako Pure Chemical Industries), Cr_2O_3 (Wako Pure Chemical Industries), a mixture of CuO and Cr_2O_3 (CuO/Cr_2O_3 = 1 and 2, molar ratio), copper chromite (CuO/Cr_2O_3, Aldrich Chemical Company, Inc.) and Ba-promoted copper chromite ($CuO/Cr_2O_3/BaO$, Aldrich Chemical Company, Inc.). Copper-based oxide commercial catalysts,

N203SD (Nikki Chemical Co.), KMB (Toyo CCI Corp.), G66B and G89 (Nissan Girdler Catalyst Co.) were also employed. Potassium methoxide solution (10 cm^3, 30% in methanol solution) was employed as an alkoxide component.

RESULTS AND DISCUSSION

The BNL Methanol Process

The performance of the BNL Ni catalysts at 373 K and 433 K is summarized in Table 1. Methanol was formed quite selectively over the BNL catalysts at 353-433 K and 1.1-5.0 MPa of initial pressure. (Experiments could not be carried out at temperatures above 433 K because the pressure started to decrease in the course of the heating process. Also, it is reported[3] that the catalyst works only below 423 K.) The maximum STY was obtained at 433 K and at 5.0 MPa because higher temperatures and higher initial pressures tended to enhance methanol productivity under the studied conditions. The STY with the BNL catalysts also varied with Ni concentration in the catalyst system and reached 0.89 kg l^{-1} h^{-1} at the optimum concentration. At 433 K, the BNL catalysts yielded almost 90% for CO conversion and over 99% for selectivity to methanol. Ni is a well-known catalyst for methanation of carbon oxides and Fischer-Tropsch synthesis. However, to the author's knowledge, it has never been reported that a Ni-based compound catalyzes methanol synthesis from $CO + H_2$. Thus, the BNL catalyst is quite novel at this point. Since the catalyst was highly active even at temperatures much lower than the operating temperature of the conventional methanol process (503-543 K), with this catalyst, it should be possible to eliminate recycling facilities for unconverted gas, which would reduce the production cost of methanol.

Small amounts of methyl formate and dimethyl ether were also produced. They were considered to be formed by the carbonylation of methanol (equation 2) and dehydration of methanol (equation 4), where produced methanol was a reactant:

$$2\ CH_3OH \rightarrow CH_3OCH_3 + H_2O \qquad (4)$$

Sodium *tert*-amyl alkoxide that could possibly be formed and exist in the catalyst system, might be responsible for equation 2 since alkoxide is known to catalyze carbonylation of methanol[7].

Figure 1 indicates the effect of methanol concentration in the catalyst system on the STY. In these experiments a certain amount (1-8 cm^3) of methanol was initially added to the catalyst system and the reaction was carried out at 373 K and 5 MPa. As shown in Figure 1, methanol addition did not affect catalytic activity significantly under the studied conditions although the STY showed a slight tendency to decrease with methanol concentration. A 99% selectivity to methanol was obtained, independent of methanol concentration. Therefore, constraints from chemical equilibrium or inhibition of the reaction by adding methanol was not recognized. On the other hand, a large amount of methyl formate was formed in the experiments with methanol addition at ambient temperature. Carbonylation of methanol (equation 2) seemed to prevail at such low temperatures, where sodium alkoxide functioned as a catalyst. Figure 2 shows the time courses of the temperature and the pressure during the multiple-charging experiment. Even when the pressure decrease became small, the pressure started to decrease again by recharging the feed gas, which suggested that the reaction continued to proceed. However, a marked pressure decrease was not observed after the second recharge of syngas (in the 3rd reaction). Methanol of 167 mmol was formed at the end of the entire reaction. Such an amount of methanol was not found to affect or inhibit the methanol productivity as shown in Figure 1. Therefore it was because of deactivation of the catalyst that only a slight pressure decrease was observed in the 3rd reaction.

To clarify the active species of the BNL catalyst, experiments with a mixture of sodium hydride and nickel acetate as a catalyst were carried out. Figure 3 shows the results. With sodium hydride and nickel acetate, methanol synthesis proceeded as well as with the BNL catalyst. The sodium hydride and nickel acetate catalyst exhibited a slightly lower STY than the BNL catalyst, but it showed almost the same value in CO conversion and selectivity as the BNL catalyst. On the other hand, in the experiments using a mixture of *tert*-amyl alcohol and sodium hydride as a catalyst (the nickel acetate component of the BNL catalyst was not employed), methanol synthesis did not occur at temperatures where the BNL catalyst works. Methyl formate and dimethyl ether were formed only when methanol was initially added into the catalyst system. Therefore, the nickel species that is activated or reduced by sodium hydride is responsible for methanol synthesis.

The BNL catalyst exhibited activity in several subsequent experiments, while a mixture of sodium hydride and nickel acetate that was employed in the previous experiment, did not show activity in the second experiment. Hence, *tert*-amyl alcohol, which is a component of the BNL catalyst and was not used in the experiments in Figure 3, may play a role in re-activating the nickel species and making the BNL catalyst function again in the subsequent reactions.

Methanol Synthesis via MF

Methanol was formed rapidly at around 373 K using a mixture of copper-based oxide and alkoxide. Figure 4 shows the STY of methanol and methyl formate at 373 K and 5 MPa with various oxides and potassium methoxide as a catalyst. It should be noted that the catalyst system initially contains methanol (*ca.* 220 mmol) because potassium methoxide in methanol solution was employed as an alkoxide component. N203SD and G89, the copper-chromite-based catalysts, showed activity for methanol among the commercial catalysts. In particular, N203SD exhibited high STY. Copper chromite (unpromoted and Ba-promoted) also had the STY values comparable to N203SD. On the other hand, methanol was consumed and only methyl formate was formed over the CuO/ZnO-based catalysts (KMB and G66B), which are the conventional catalysts for methanol synthesis . Since all the oxides exhibiting high activity for methanol were copper-chromite-based compounds, it was considered that copper chromite is quite effective for methanol synthesis *via* MF. It is generally known that copper chromite promotes hydrogenation of carbonyl compounds. Thus, in this study,

copper chromite might catalyze hydrogenolysis of methyl formate that resulted from carbonylation of methanol.

When CuO or Cr_2O_3 was employed as an oxide component, only methyl formate was formed with consumption of methanol, which suggested the progress of carbonylation of methanol. However, amounts of methanol and methyl formate were produced using a mixture of both. Thus it is suggested that an active site for hydrogenolysis of methyl formate might be yielded by mixing of CuO and Cr_2O_3.

Figure 5 shows the dependence of the STY on temperature and initial pressure using N203SD and potassium methoxide. Methanol was formed rapidly and selectively over 353 K (CO conversion: 87-94%, selectivity to methanol: 87-98%). However, a significant amount of methyl formate was formed at ambient temperature, which indicated carbonylation of methanol proceeded rapidly at such low temperature. As seen in the figure, higher temperatures and higher initial pressures enhanced methanol productivity, while lower temperatures and higher pressures increased methyl formate formation.

The STY Evaluation of Low-Temperature Methanol Synthesis

The STY of low-temperature methanol synthesis and that of the conventional methanol production process are compared in Figure 6. In the conventional process[8], copper-zinc-based oxide catalysts ($CuO/ZnO/Al_2O_3$ or $CuO/ZnO/Cr_2O_3$) are employed under the conditions of temperature of 503-573 K, pressure of 5-20 MPa, and space velocity of 10,000-40,000 h^{-1}. In the ICI process, a typical methanol process, the STY of 0.5-0.77 kg l^{-1} h^{-1} (average 0.66 kg l^{-1} h^{-1}) is obtained under the conditions of 500-523 K and 5-10 MPa. The BNL process showed the STY of 0.89 kg l^{-1} h^{-1} at the optimum Ni concentration (433 K, 5 MPa), which was almost the same value as that in the ICI process. Thus, the BNL process has the possibility of producing methanol more efficiently than the conventional process. On the other hand, methanol synthesis *via* MF showed the STY of 0.13 kg l^{-1} h^{-1} at 423 K and 5 MPa (feed: $H_2/CO = 1$), which is 1/5 of the STY in the ICI process. However, the STY is expected to be improved by optimizing reaction conditions and catalyst concentration in the liquid phase, and by searching for an active catalyst system.

CONCLUSIONS

Low-temperature methanol synthesis in the liquid phase has been studied and its possibility as an industrial process was evaluated in terms of the STY. Methanol productivity comparable to that of the conventional methanol process is anticipated under much milder conditions by using the BNL catalyst. It was suggested, however, that extension and stability of the catalyst life are the important subjects in the BNL process. Methanol synthesis *via* MF also showed activity for methanol at low temperatures but its productivity was still quite low. It is necessary to explore an active catalyst system and examine the catalytic behavior in more detail to improve the STY value.

REFERENCES

(1) Deane, A. A., Huber, D. A. and DeRosa, J., "Coproduction of Methanol and Electricity"; EPRI Report AP-3749 (1984).
(2) Mahajan, D. and Sapienza, R. S., "Proceedings: 15th Annual EPRI Contractors' Conference on Fuel Science"; EPRI Report GS-7434 (1991).
(3) Sapienza, R. S., Slegeir, W. A., O'Hare, T. E. and Mahajan, D., U.S. Patent 4,614,749, 4,619,946, 4,623,634 (1986).
(4) Sørum, P. Å. and Onsager, O. T., *8th Int. Congr. Catal.*, vol. II, 233 (1984).
(5) Gormley, R. J., Rao, V. U. S., Soong, Y. and Micheli, E., *Appl. Catal. A: General*, 87, 81 (1992).
(6) Palekar, V. M., Tierney, J. W. and Wender, I., *Appl. Catal. A: General*, 103, 105 (1993)
(7) Gormley, R. J., Giusti, A. M., Rossini, S. and Rao, V. U. S., *9th Int. Congr. Catal.*, vol. II, 553 (1988).
(8) Hermann, R. G., Klier, K., Simmons, G. W., Finn, B. P., Bulko, J. B. and Kobylinski, T. P., *J. Catal.*, 56, 407 (1979).

Table 1. Catalytic activity for low-temperture methanol synthesis over BNL Ni catalysts.

Temp. (K)	P[a] (MPa)	Time (h)	Ni conc.[b] (mol l^{-1})	Conv.[c] (%)	Select.[d] (%)	Products[e] (mmol) MeOH	Me_2O	$HCOOCH_3$	CO_2	CH_4	H.C.	STY (kg-MeOH $l^{-1}h^{-1}$)
373	1.1	1	94.6	80.0	93.4	54.4	0.001	0.662	0.059	trace	---	0.016
373	3.0	1	94.6	60.3	98.4	50.7	trace	0.403	---	0.003	---	0.024
373	5.0	1	94.6	87.8	99.5	140	0.010	0.353	0.017	---	---	0.043
433	1.6	1	94.6	86.7	99.3	33.0	trace	0.049	---	0.005	---	0.025
433	3.0	1	94.6	95.5	99.8	98.8	0.013	0.046	---	0.004	---	0.12
433	5.0	1	94.6	90.7	99.8	203	0.017	0.237	---	0.004	---	0.25
433	5.0	1	23.7	98.9	99.7	213	0.196	0.031	---	0.004	0.026	0.24
433	5.0	1	94.6	90.7	99.8	203	0.017	0.237	---	0.004	0.001	0.25
433	5.0	1	94.6	93.0	99.9	237	0.044	0.025	---	0.007	0.004	0.47
433	5.0	1	180	96.3	99.1	257	0.378	0.777	---	0.005	0.005	0.89
433	5.0	1	284	88.6	99.0	136	trace	0.588	0.132	0.005	---	0.41

Catalyst: NaH/*tert*-amyl alcohol/$Ni(CH_3COO)_2$. Catalyst amount = 2.5-30 mmol as $Ni(CH_3COO)_2$. Volume of solvent = 50-100 cm^3.
[a]Initial pressure at ambient temperature. [b]Ni concentration in the catalyst system.
[c]Conversion of carbon monoxide. [d]Selectivity to MeOH.
[e]Products: Me_2O = dimethyl ether; H.C. = hydrocarbons except CH_4.

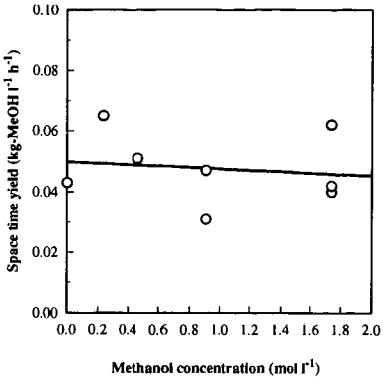

Figure 1. Effect of methanol addition on space time yield over BNL Ni catalysts Catalyst: NaH/*tert*-amyl alcohol/Ni(CH$_3$COO)$_2$. Catalyst amount: 10 mmol as Ni(CH$_3$COO)$_2$. Solvent: triglyme (100 cm^3). Reaction conditions: temperature = 373 K, initial pressure = 5 MPa, H$_2$/CO = 2.

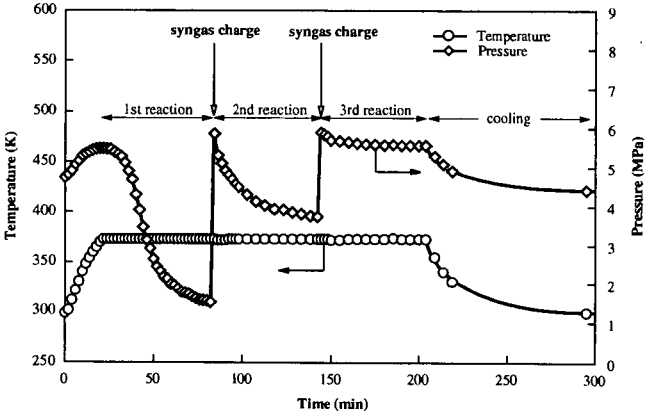

Figure 2. Temperature and pressure profiles using a BNL Ni catalyst (multiple-charging experiment). Catalyst: NaH/*tert*-amyl alcohol/Ni(CH$_3$COO)$_2$. Catalyst amount: 10 mmol as Ni(CH$_3$COO)$_2$. Solvent: triglyme (100 cm^3). Reaction conditions: initial pressure = 5.0 MPa, reaction temperature = 373 K.

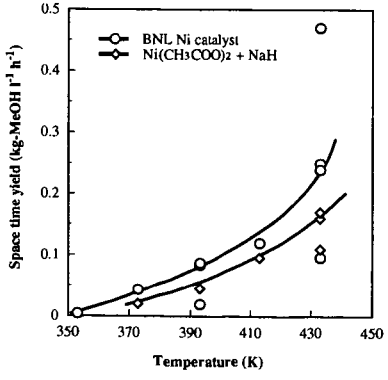

Figure 3. Space time yield over BNL Ni catalysts and nickel acetate + sodium hydride catalysts. Catalyst amount: 10 mmol as Ni (CH$_3$COO)$_2$. Solvent: triglyme (100 cm^3). Reaction conditions: initial pressure = 5 MPa, H$_2$/CO =2.

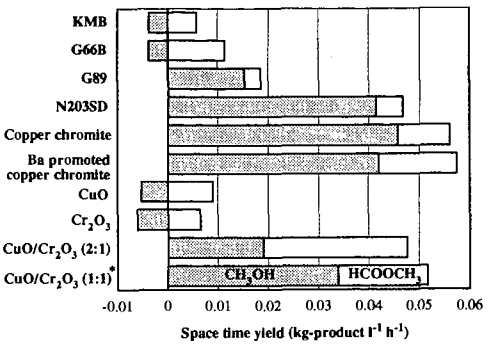

Figure 4. Space time yield over a mixture of metal oxide and potassium methoxide. Catalyst: metal oxide 4 g (* 6 g) + CH_3OK 10 cm^3 (30% in methanol solution). Solvent: triglyme (90 cm^3). Reaction conditions: reaction temperature = 373 K, initial pressure = 5.0 MPa (at ambient temperature), H_2/CO = 2.

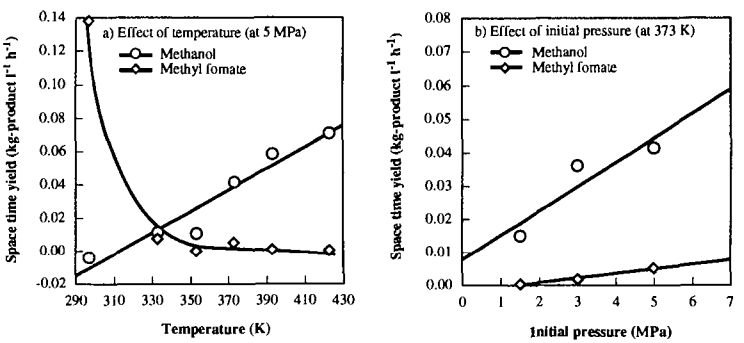

Figure 5. Effect of reaction parameters on space time yield for low-temperature methanol synthesis *via* methyl formate a) Effect of temperature (initial pressure: 5 MPa), b) Effect of initial pressure (reaction temperature: 373 K). Catalyst: N203SD 4 g + CH_3OK 10 cm^3 (30% in methanol solution). Solvent: triglyme (90 cm^3). Feed gas: H_2/CO = 2.

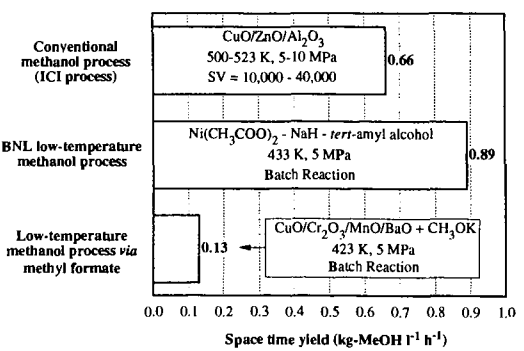

Figure 6. Space time yield of various methanol synthesis technologies